Kodak Color Control Patches

Kodak Gray Scale

報告番号 乙第 5536 号

Variable Structure System Theory Based Identification and Control for the Systems with Uncertainties

Xinkai Chen

Summary

Variable Structure System (VSS) control is a well-known solution to the problems of the deterministic control of uncertain systems because of its excellent robustness and invariance properties. The characterizing feature of VSS control is sliding motion, which occurs when the system state repeatedly crosses certain subspaces (sliding surfaces) in the state space. A VSS controller may comprise nonlinear and linear parts, and has been well studied in the literature. The VSS control and allied techniques are also widely used in model-following and model reference adaptive control, tracking control and observer systems. Thousands of papers and numerous practical industrial applications using VSS techniques have been appeared in these years. But there still remain many interesting and important problems.

First, this thesis deals with the implementation problems by a digital computer for a well designed linear continuous-time variable structure control system. By using the zero-order-hold of the designed continuous-time VSS controller, a corresponding discrete-time controlled system is obtained. For the discrete-time system, a new definition, which is called "discrete-time weak-pseudo-sliding mode", is given to describe the zigzag behavior corresponding to the continuous-time VSS sliding mode. An upper bound of the sampling period is given to guarantee the existence of the weak-pseudo-sliding mode along the prescribed surface for the discrete-time system. If the chosen sampling period is not greater than this upper bound, the zero-order-hold of the continuous-time VSS controller can still stabilize the sampled data system without any modification.

Second, a discrete robust quasi-sliding mode adaptive controller is presented for the system with model uncertainties, unmodeled dynamics and bounded disturbances.

The proposed method is adaptive control in conjunction with a sliding mode based controller design. The bounded motion of the state around the sliding surface and the stability of the global system in the sense that all signals remain bounded are guaranteed. In the proposed adaptive algorithms, the dead-zone method is employed even though the upper and lower bounds of the disturbances are unknown. If some information of the perturbations is known, the controller can be modified to improve the performance of the controlled systems.

Then, based on the VSS theory, a new method of estimating the disturbance is presented for minimum-phase (with respect to the relation between the disturbance and output) continuous-time dynamical systems with arbitrarily relative degrees. By using the transfer function method, first, the higher order filter of the disturbance is estimated; then, the lower order filter of the disturbance is estimated inductively; eventually, the disturbance is estimated. In order to be implemented by a digital computer, the discontinuous estimates are approximately modified by differentiable functions. Detailed tests of the parameters are also presented by computer simulations. Then the disturbance identification algorithm is extended to a class of nonminimum phase dynamical systems. The estimated disturbance is also employed to construct a state observer and a pole assignment controller. In order to show the practicality of the new disturbance estimator, it is employed to control a linear motor. Moreover, experiment results show that the new observer is superior to the traditional disturbance observer when the impulse disturbances exist.

Consequently, based on the VSS theory, this thesis presents a new method of estimating the disturbances (or system nonlinearities and any model uncertainties) for continuous-time multi-input multi-output (MIMO) minimum phase (with respect to the relation between the disturbance and the output) dynamical systems. The designed robust method requires only the input and output measurements of the system. Even for the MIMO systems with the assumption that the partial states directly affected by the disturbances do not directly appear in the outputs (when it is considered in the state space), the disturbances can also be estimated by applying the proposed formulation. The estimated disturbances are then employed to construct a

robust state observer. Further, the estimated disturbances and the state observer are applied to synthesize a controller to place the desired stable poles and to cancel the disturbances.

Finally, this thesis presents implicit robust state observers for uncertain dynamical systems with arbitrarily relative degrees (with respect to the relation between the disturbance and the output). For systems with relative degree one, the state is expressed by the filters of the input and the output. No *a priori* knowledge of the disturbance is required in this case. For systems with higher relative degrees, the state vector is asymptotically expressed by the filters of the input, the filters of the output and the estimates of the first order filters of the disturbance. Then, the state observer and the estimated disturbance are applied to a controller to place desired poles and to cancel the disturbance. The obtained results are also extended to MIMO uncertain systems.

Contents

Chapter 1

Introduction

Mathematical models of actual systems contain uncertainty terms which reflect the designer's lack of knowledge about parameter values and disturbances. Such poorly known quantities may be assumed to be constant or time-varying. Uncertainties arising from imperfect knowledge of system inputs and inaccuracies in the mathematical modeling itself, contribute to performance degradation of the feedback control systems.

Almost all controller design procedures are based on the models of one form or another. It is of great practical importance that the controller performs well when the dynamical behavior of the real process differs from that described by its model. The attribute "robust" will be used for a property which holds not only for the model but also in the presence of model uncertainties. In order to accomplish this objective, not only must a process model and the performance specifications be provided for the design, but also some indication of the model accuracy should be made. However, in a number of instances, the plant to be controlled is too complex and the basic physical processes in it are not fully understood. Control design techniques then need to be augmented with an identification technique aimed at obtaining a progressively better understanding of the plant (such as the state, the parameters, the disturbances, etc.) to be controlled. Thus, the identification of the system uncertainties is of great importance in the robust control formulations. This thesis discusses the

identification and the robust controller design problems for the systems with uncertainties.

1.1 Introduction of the VSS Theory

The deterministic control of uncertain time-varying systems proposes the use of straightforward fixed nonlinear feedback control functions, which operate effectively over a specified magnitude range of system parameter variations and disturbances, without any on-line identification of the system [21,70,71]. An immediate advantage of such an approach is that no statistical information of the system variations is required to yield the desired dynamical behavior, and robustness is achieved, not in an average sense, but for all possible values of the underlying uncertainty. Furthermore, if the parameter variations satisfy certain matching conditions, complete insensitivity to system variations can be achieved. The main area of application of deterministic control of uncertain systems include electric motor drives, robotics, flight control, space systems, power electronics, chemical processes, automotive control systems and magnetic levitation [23,41,44,45,47,55,58,64,65,67]

The two main approaches to deterministic robust control of uncertain systems are the Sliding Mode Control (SMC) technique using a special behavior of variable structure systems; the second approach is known as the Lyapunov control design technique [21,70,71]. The outstanding feature of these controllers is their excellent robustness and invariance properties. In this thesis, the first approach will be discussed.

The essential property of Variable Structure System (VSS) control is that the discontinuous feedback control switches on one or more surfaces in the state space [9,26,54-58]. Thus the structure of the feedback system is altered or switched as the state crosses each discontinuity surface. Sliding motion occurs when the system state repeatedly crosses and immediately re-crosses a switching surface, because all motion in the neighborhood of the surface is directed inwards towards the surface. Following an initial trajectory onto the switching (sliding) surfaces, the system state is

constrained to lie upon these surfaces and is said to be in the sliding mode. In the sliding mode the system is totally invariant to a class of matched disturbances and parameter variations with known upper and lower bounds; the decoupled system dynamics then being wholly described by the reduced order dynamics of the selected sliding surfaces [57]. In the sliding mode the control element has high (theoretically) gain, while the control actually passed onto the plant takes finite values.

The discontinuous controller can be replaced in many practical applications with continuous nonlinear control which yield a dynamical response arbitrarily close to the discontinuous controller, but without undesirable chatter motion [48]. Following an initial trajectory onto the switching (sliding) surfaces, the system state is constrained to lie in a neighborhood of these surfaces.

VSS control with a sliding mode was first studied intensively in the 1960s by Russian authors [16,55], notably Emel'yanov and Utkin, although early work was also done by Flügge-Lotz in the 1950s [17]. In recent years the subject has attracted the attention of numerous researchers. The basic interest in the technique stems because of its applicability to linear and nonlinear dynamical systems as well as to systems with delays and distributed parameters [20]. VSS control is particularly well suited to the deterministic control of uncertain control systems. Some of the major interest have been the use of VSS control and allied techniques in model-following and model reference adaptive control, tracking control and observer systems [10,11,23,24,59].

The main characteristic in VSS control is to force the state trajectory of the system to reach a desired surface containing the origin of the state-space, stay within that hyperplane thereafter and approach the origin. The latter behavior is called *sliding* and the system is said to be in a *sliding mode* (SM) [57] .

1.1.1 The Concept of VSS Theory

The basic philosophy of the variable structure approach is simply explained by contrasting it with the linear state regulator design for the single-input system

$$\dot{x} = Ax + bu \tag{1.1}$$

In the linear state regulator design, the structure of the state feedback is fixed as

$$u = k^T x \tag{1.2}$$

where the constant parameters are chosen according to various design procedures, such as eigenvalue placement or quadratic minimization. In variable structure systems, the control is allowed to change its structure, i.e. to switch at any instant from one to another member of a set of possible continuous functions of the state. The variable structure design problem is then to select the parameters of each of the structures and to define the switching logic. A reward for introducing this additional complexity is the possibility to combine useful properties of each of the structures. Moreover, a variable structure system can posses new properties not present in any of the structure used. For instance, an asymptotically stable system may consist of two structures neither of which is asymptotically stable. This possibility is illustrated by some examples [54].

As the first example, a second-order system is considered to explain the VSS theory.

$$\ddot{x} = -\Psi x \tag{1.3}$$

This system have two structures defined by $\Psi = \alpha_1^2$ and $\Psi = \alpha_2^2$. The phase portrait consists of families of ellipses (Fig. 1.1(a), (b)) and hence, neither structure is

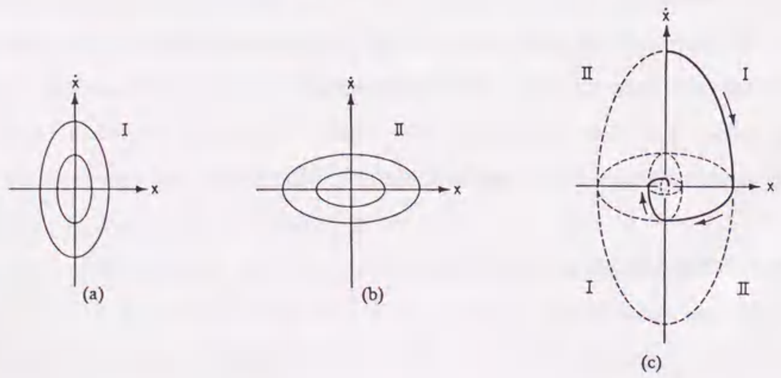

Fig. 1.1 Asymptotically stable VSS consisting of two stable structures

asymptotically stable. However, asymptotic stability can be achieved if the structure of the system is changed on the coordinate axes, that is , if the switching logic is

$$\Psi = \begin{cases} \alpha_1^2 & if\ x\dot{x} > 0 \\ \alpha_2^2 & if\ x\dot{x} < 0 \end{cases} \tag{1.4}$$

The resulting phase portrait is shown in Fig. 1.1(c).

In the second example, the system

$$\ddot{x} - \xi\dot{x} + \Psi x = 0\,, \qquad \xi > 0 \tag{1.5}$$

is considered, where the linear structure corresponds to negative and positive feedback when Ψ is equal to either $\alpha > 0$ or $-\alpha$. Both structures are unstable (Fig. 1.2(a),(b)). Note that the only motion converging to the origin is along the stable eigenvector of the structure with $\Psi = -\alpha$. If the switching occurs on this line and on $x = 0$ with the switching law

$$\Psi = \begin{cases} \alpha, & if\ xs > 0 \\ -\alpha, & if\ xs < 0 \end{cases} \tag{1.6}$$

where

$$s = cx + \dot{x}\,, \quad c = \lambda = -\frac{\xi}{2} \pm \sqrt{\frac{\xi^2}{4} + \alpha} \tag{1.7}$$

then the resulting VSS will be asymptotically stable.

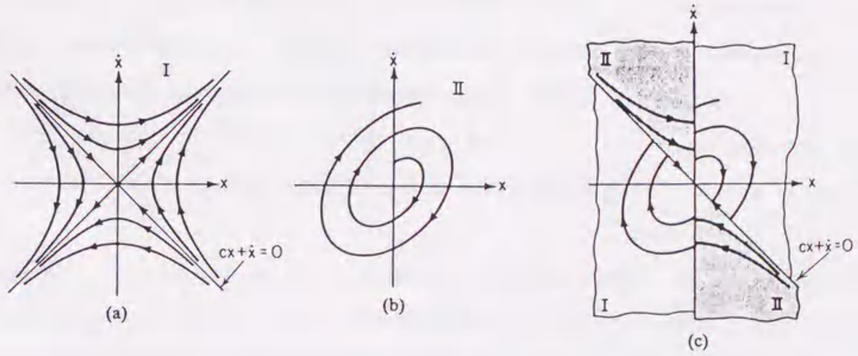

Fig. 1.2 Asymptotically stable VSS consisting of two unstable structures

In the above two examples, new system properties are obtained by composing a desired trajectory from the parts of trajectories of different structures.

Now, the general description of VSS is given by the next definition [57].

Definition 1.1 Consider the system described by

$$\rho x = f(x,u,t),\ \ x \in R^n,\ \ u \in R^m \tag{1.8}$$

where ρ denotes the differential operator or the advance operator as the case may be. The *variable structure system control* is:

1) Design a switching surface $s(x) = 0$ to represent a desired system dynamics, which is of lower order than the given plant.

2) Design a variable structure control

$$u(x,t) = \begin{cases} u^+(x,t) & as \quad s(x) > 0 \\ u^-(x,t) & as \quad s(x) < 0 \end{cases} \tag{1.9}$$

such that any state outside the switching surface is driven to reach the surface in finite time.

1.1.2 The Sliding Mode for a Continuous-Time System

In the above examples, an even more fundamental aspect of VSS is the possibility to obtain trajectories not inherent in any of the structures. These trajectories describe a new type of motion "*sliding mode*" (SM) [54].

To shown how such motion occurs let us reconsider the second example using $0 < c < \lambda$ inside of $c = \lambda$ (Fig. 1.3). The phase trajectories are directed towards the switching line $s = cx + \dot{x} = 0$ and hence once on this line the state must remain on it. The motion along a line which is not a trajectory of any of the structure is called the *sliding mode*.

The equation

$$\dot{x} + cx = 0 \tag{1.10}$$

determines the behavior of the system in the sliding mode. It is useful to note that this behavior depends on the parameter c. This invariance with respect to plant

parameters is of extreme importance when controlling plants.

Definition 1.2 [see 57] Consider the system (1.8), where ρ is the differential operator. The continuous-time *sliding mode* is:

The state $x(t)$ is driven to the surface $s(x) = 0$ in a finite time. On the switching surface, the behavior of system (1.8) is governed by the desired dynamics.

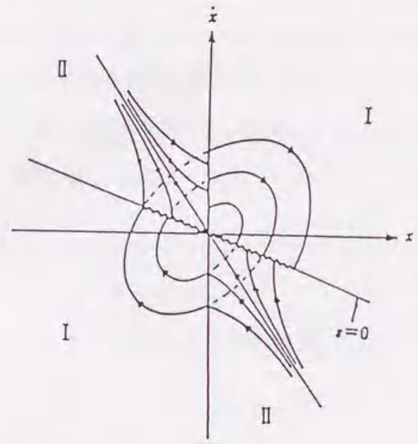

Fig. 1.3 Sliding mode in a second order VSS

Remark 1.1 It should be noted that a variable structure control system can be devised without a sliding mode (for example, Fig. 1.2), but such a system does not posses the associated merits of the sliding mode.

1.1.3 The Pseudo-Sliding Mode for a Discrete-Time System

It is obvious that the definition for continuous-time sliding modes can not be applied to the discrete-time sliding modes since the concept of velocity vectors of the system trajectories is not available. The switching frequency is actually equal to or lower than the sampling frequency. The comparatively low switching frequency causes the

discrete-time system state to move about the switching surface in a zigzag manner.

So, the similarity between discrete-time sliding modes and continuous-time sliding modes disappears as the sampling period increases with the system trajectory appearing to zigzag within a bounded domain. Thus, how to define discrete-time sliding mode is an open question. Various kinds of definitions have been given to describe the behavior of this particular motion [2,18,38,49,69,71]. Among these definitions, "*pseudo-sliding mode*" (PSM)([69,71]) may be the most precise statement.

Definition 1.3 (see Fig. 1.4) Consider the dynamical system (1.8), where ρ is the advance operator. The system is said to exhibit a pseudo-sliding mode along the surface $s(k)$ in R^n if there exists an integer $K>0$, such that for all $k>K$,

$$x(k) \in \Omega_s \tag{1.11}$$

where Ω_s is defined as

$$\Omega_s = \{x: \|s(k)\| < \varepsilon \ , \ \varepsilon > 0\}. \tag{1.12}$$

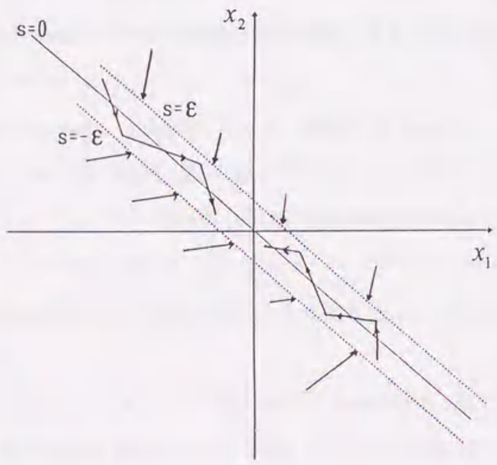

Fig. 1.4 Discrete-time pseudo-sliding mode

Remark 1.2 Further discussions on the discrete-time sliding mode will be given in Chapter 2 of this thesis.

1.1.4 The Equivalent Control

Assume the sliding mode exists on the surface $s(x)=0$. Let us find a continuous control such that under the initial position of the state vector on this surface, it yields identical equality to zero of $\rho s(x)$ along the system (1.8) trajectories:

$$\rho s(x) = Gf(x,u,t) = 0 \tag{1.13}$$

where the rows of the $m \times n$ matrix $G = \{\partial s / \partial x\}$ are the gradients of the functions $s_i(x)$.

Assume that a solution (or a number of solutions) of the system of the algebraic Equation (1.13) with respect to the control $u(t)$ does exist. Substituting this solution, hereafter referred as *equivalent control* $u_{eq}(x,t)$, in system (1.8) to replace u yields

$$\rho x = f(x,t,u_{eq}) \tag{1.14}$$

It is obvious that, by virtue of condition (1.13), a motion starting in $s(x(t_0))=0$ will proceed along the trajectories which lie on the surface $s(x)=0$.

The above procedure will be called the equivalent control method and Equation (1.14) obtained as a result of applying this method will be regarded as the sliding equation describing the motion on the intersection of discontinuity surface $s(x)=0$. Usually, the equivalent control satisfies [46,57]

$$u^-(x,t) < u_{eq} < u^+(x,t) \tag{1.15}$$

For the continuous-time systems, it can be explained from the geometric viewpoint. The equivalent control method implies a replacement of the undefined discontinuity control on the discontinuity boundary with a continuous control which directs the velocity vector in the system state space along the discontinuity surface intersection.

For example, in order to find this vector in a system with a single discontinuity surface $s(x)=0$ at some point (x,t) (Fig. 1.5) one should vary the scalar control from u^- to u^+, plot the locus of $f(x,t,u)$ and find the point where it intersects the tangential plane. The point of intersection determines the equivalent control $u_{eq}(x,t)$ and the right hand part $f(x,t,u_{eq})$ of the sliding mode Differential Equation (1.14) (where ρ represents the differential operator).

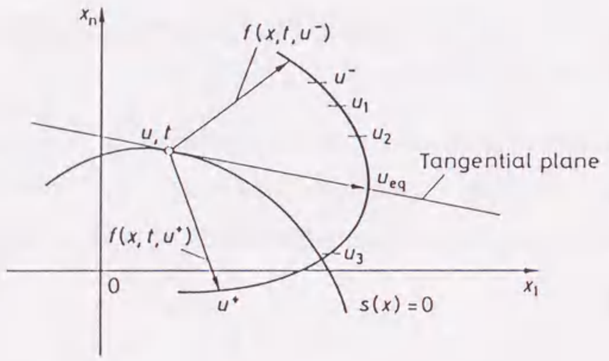

Fig. 1.5 The geometric explanation of the equivalent control for a continuous-time system.

Consider now the equivalent control procedure for an important particular case of a nonlinear discontinuous system, the right hand part of whose differential equation is a linear function of the control

$$\rho x = f(x,t) + B(x,t)u \tag{1.16}$$

where $f(x,t)$ and $B(x,t)$ are all argument continuous vector and matrix of dimension $n\times 1$ and $n\times m$, respectively, and the control discontinuous control u changes in compliance with (1.9). The equivalent control Equation (1.13) for the case (1.16) can be written as

$$\rho s = Gf + GBu = 0 \tag{1.17}$$

Assuming that the matrix GB is nonsingular for all x and t, the equivalent control can be found as

$$u_{eq}(x,t) = -[GB]^{-1}Gf \tag{1.18}$$

Now, substituting of this control into (1.16) yields

$$\rho x = f - B(GB)^{-1}Gf \tag{1.19}$$

which describes the sliding mode motion on the surface $s=0$.

1.2 Scope of the Thesis

This thesis discusses the identification and robust control problems for uncertain systems based on VSS theory. The originalities of this thesis are:

1) The digital implementation of the continuous-time variable structure control systems has been solved. An upper bound of the sampling period is given to assure the stability of the sampled-data system by using the zero-order-hold of the well-designed continuous-time control.

2) For the discrete-time systems with uncertainties, an adaptive quasi-sliding mode controller, which makes the best use of the merits of adaptive method and sliding mode approach, is given to stabilize the system. Also, a new adaptive algorithm with dead-zone for estimating the unknown parameters is derived even though the upper and lower bounds of the disturbances are unknown.

3) For the continuous-time minimum phase dynamical systems with arbitrarily relative degrees, the disturbance is identified by using the VSS theory. Also, the disturbance estimation problem is solved by introducing approximate inverse systems for a class of nonminimum phase systems with arbitrarily relative degrees. While the disturbance can be identified only for the minimum phase systems with relative degree one traditionally, not to say the nonminimum phase systems with arbitrarily relative degrees.

4) For the MIMO minimum phase systems with arbitrarily relative degrees, the disturbances are estimated based on the VSS equivalent control theory, while the disturbance identification problems has never been considered for the MIMO uncertain systems until now. A state observer is formulated for the first time for the MIMO systems with arbitrarily relative degrees.

5) For the uncertain systems with arbitrarily relative degrees, implicit state observers are formulated, while the state observer can only be formulated by appealing to discontinuous approaches for the minimum phase uncertain systems with relative degree one traditionally.

The organization of this thesis is as follows. Chapter 2 deals with the digital implementation problem of a well-designed continuous-time variable structure systems with sliding modes since almost all controllers are implemented by digital computers nowadays. Chapter 3 gives an adaptive quasi-sliding mode controller for discrete-time systems with model uncertainties, unmodeled dynamics and bounded disturbances. In Chapter 4, first, the disturbance is identified for minimum phase systems; then, the formulation is extended to a class of nonminimum phase systems; consequently, the applications of the estimated disturbance are discussed. In Chapter 5, the disturbance estimation and its application problems are considered for the complicated MIMO uncertain systems. In Chapter 6, implicit state estimators and their applications are presented for SISO systems as well as MIMO systems. Chapter 7 summarizes this thesis and remarks the future research subjects.

Chapter 2

Computer-Controlled Continuous-Time Variable Structure Systems with Sliding Modes

2.1 Introduction

Variable Structure Control has been studied for more than 30 years and has been applied in many different fields. But the main theoretical development has been focused on the continuous-time systems. Its digital counter-part, discrete-time variable structure control, has received less attention. So, the problems associated with the implementation of a well designed continuous-time VSC by digital computer have to be solved [33]. Among these problems, the selection of the sampling period to guarantee the discrete-time sliding on the prescribed sliding surfaces may be the most important one. It might be argued that if the sampling period is chosen to be small enough, the zero-order-hold of the continuous-time VSC structure can still be used as an effective input of the sampled data system. And this input may result in a discrete-time sliding mode along the prescribed hyperplane. Further, the stability of the controlled sampled data system can also be preserved. In this paper, we will discuss the sampling period selection and the stability problem of the digital implementation of the continuous-time variable structure control systems.

In the continuous-time systems, the existence of sliding mode implies that in a

vicinity of the prescribed switching surface, the velocity vectors of the state trajectories always point towards that surface. This requires infinitely fast switching. But in the discrete-time systems, as the concept of velocity vectors is not available, the switching frequency is equal to or lower than the sampling frequency. This causes the discrete-time system state to move about the switching surface in a zigzag manner. Thus, how to define discrete-time sliding mode is an open question.

Consider the single-input discrete-time dynamic system

$$x(k+1) = f(k, u(k), x(k)) \tag{2.1}$$

where $x(k) \in R^n$, $u(k)$ is the control input. The switching surface is defined as $s(k) = s(x(k)) = 0$.

Discrete-time sliding mode was first named "quasi-sliding mode" by Milosavljevic [35] who gave a necessary condition for the existence of the sliding mode by replacing the derivative term in the well-known condition $\lim_{s \to 0} \dot{s}(t) \cdot s(t) < 0$ for the continuous-time system with a forward difference

$$\lim_{s(k) \to 0^+} \nabla s(k) < 0, \qquad \lim_{s(k) \to 0^-} \nabla s(k) > 0 \tag{2.2}$$

where $\nabla s(k) = s(k+1) - s(k)$. It is obvious that the conditions are rarely satisfied in practice, since it is impossible for a discrete-time system to approach a switching surface sufficiently closely.

As the similarity between the discrete-time sliding modes and the continuous-time sliding modes disappears as the sampling period increases, "pseudo-sliding mode" may be a more precise statement of this phenomenon [66,71].

Definition 2.1 The system (2.1) is said to exhibit a pseudo-sliding mode on the surface $s(k) = 0$ if in an open neighbourhood of the surface $s(k) = 0$, the condition

$$\nabla s(k) \cdot s(k) < 0 \tag{2.3}$$

holds, where $\nabla s(k) = s(k+1) - s(k)$.

Sarpturk *et al* [42] proposed a sufficient condition for the occurrence of the so-called "pseudo-sliding mode".

$$|s(k+1)| < |s(k)| \tag{2.4}$$

The above condition actually imposes upper and lower bounds on the discrete-time variable structure control systems. Kotta [29] pointed out that the upper and lower bounds depend on the distance of the system state from the sliding surfaces. The condition (2.4) can be equivalently replaced by $s^2(k+1) < s^2(k)$ [18] or $|s(k) \cdot s(k+1)| < s^2(k)$ [46].

As shown in [49] and [66], the condition (2.4) and its equivalents are only sufficient conditions for the existence of pseudo-sliding mode. It is not necessary to satisfy the condition (2.4) and its equivalents while $s(k) \cdot s(k+1) < 0$. In [66], a more precise definition, which is called "pseudo-sliding mode", was given to describe the zigzag behavior within a bounded domain.

Definition 2.2 The system (2.1) is said to exhibit a pseudo-sliding mode along a hyperplane $s(k) = 0$ in R^n if there exists an integer $K > 0$, such that for all $k > K$,

$$x(k) \in \Omega_s \triangleq \{x : |s(k)| < \varepsilon \|x(k)\|, \varepsilon > 0\} \tag{2.5}$$

In practice, the above definition can not easily be satisfied. On the other hand, to preserve the stability of the control systems, it is not necessary that the state $x(k)$ meets (2.5) for all $k > K$. Here, a new definition, which is called "weak-pseudo-sliding mode", will be given in Definition 2.3. It may present the best description of the zigzag phenomenon.

Definition 2.3 The system (2.1) is said to exhibit a weak-pseudo-sliding mode along a hyperplane $s(k) = 0$ in R^n if there exists a sequence $\{k_i : i = 1, 2, 3, \cdots\}$, such that

$$|s(k_i)| < \varepsilon \|x(k_i)\|_1 \tag{2.6}$$

and for $k_{i+1} > k > k_i$

$$|s(k)| \geq \varepsilon \|x(k)\|_1 \text{ and } |s(k+1)| < |s(k)| < \varepsilon \|x(k_i)\|_1 \tag{2.7}$$

where $\varepsilon > 0$.

When $k_{i+1} = k_i + 1$ are satisfied for all $i = 1, 2, 3 \cdots$, Definition 2.3 implies

Definition 2.2. Thus, Definition 2.2 can be regarded as a particular case of Definition 2.3.

This chapter is organized as follows. Section 2.2 states the background of the problem. The continuous-time Variable Structure Control System is introduced. In section 2.3, an upper bound of the sampling period is estimated to guarantee the weak-pseudo-sliding mode along the hyperplane, and the stability of the sampled data system is also investigated. In section 2.4, simulation results are presented to show the effectiveness of the selection of the upper bound of the sampling period.

In this chapter, for a matrix $A \in R^{m\times n}$, $A=[a_{ij}]$, the norms $\|A\|_1$ and $\|A\|_\infty$ are defined as

$$\|A\|_1 = \max_{1\le j\le n}\sum_{i=1}^{m}|a_{ij}|, \qquad \|A\|_\infty = \max_{1\le i\le m}\sum_{j=1}^{n}|a_{ij}| \tag{2.8}$$

2.2 Variable Structure Control for Continuous-Time Systems

For simplicity, consider the single input linear continuous-time system in the controllable canonical form

$$\dot{x}(t) = Ax(t) + bu(t) \tag{2.9}$$

where $u(t)$ is a scalar input, $x(t)$ is an n-state vector, and

$$A=\begin{bmatrix} 0 & 1 & 0 & \cdots & 0 \\ 0 & 0 & 1 & \cdots & 0 \\ \cdot & \cdot & \cdot & \cdots & \cdot \\ 0 & 0 & 0 & \cdots & 1 \\ -a_1 & -a_2 & -a_3 & \cdots & -a_n \end{bmatrix}, \qquad b=\begin{bmatrix} 0 \\ \cdot \\ \cdot \\ \cdot \\ 0 \\ 1 \end{bmatrix} \tag{2.10}$$

Assumption 2.1 The state vector $x(t)$ is available.

Assumption 2.2 a_i are unknown, but their corresponding upper bounds β_i and lower bounds α_i are known. ($\alpha_i \le a_i \le \beta_i$).

The desired switching hyperplane is defined by

$$s(t) = c_1x_1 + c_2x_2 + \cdots + c_nx_n \tag{2.11}$$

where $c_n = 1$. We denote $c=[c_1, c_2, \cdots, c_{n-1}, 1]$ and $\underline{c}=[c_1, \cdots, c_{n-1}]$, where c is chosen such that the matrix

$$\Gamma=\begin{bmatrix} 0 & 1 & 0 & \cdots & 0 \\ 0 & 0 & 1 & \cdots & 0 \\ \cdot & \cdot & \cdot & \cdots & \cdot \\ 0 & 0 & 0 & \cdots & 1 \\ -c_1 & -c_2 & -c_3 & \cdots & -c_{n-1} \end{bmatrix} \tag{2.12}$$

is stable.

The variable structure control law is considered as

$$u(t) = -c_1x_2(t) - \cdots - c_{n-1}x_n(t) - \sum_{i=1}^{n}\{\psi_i(t)+\delta\}x_i(t)\,\mathrm{sgn}\{x_i(t)\cdot s(t)\} \tag{2.13}$$

where

$$\psi_i(t) = \begin{cases} -\alpha_i, & x_i(t)\cdot s(t) > 0 \\ \beta_i, & x_i(t)\cdot s(t) < 0 \end{cases} \tag{2.14}$$

and δ is a positive constant.

Now, the stability of the controlled system will be investigated. First, we will prove that $s(t)\to 0$ as $t\to\infty$. The Lyapunov-like function is chosen as

$$V(t) = s^2(t) \tag{2.15}$$

Thus, differentiating $V(t)$ along the controlled system (2.9) and (2.13) yields

$$\dot{V}(t) = 2s(-a_1x_1 - \cdots - a_nx_n - \sum_{i=1}^{n}(\psi_i+\delta)x_i\,\mathrm{sgn}(x_is))$$

$$\le -2\delta|s(t)|\sum_{i=1}^{n}|x_i(t)| \tag{2.16}$$

By employing the fact

$$|s(t)| \le \|c\|_\infty \|x(t)\|_1 \tag{2.17}$$

(2.16) gives

$$V(t) \le -\frac{2\delta}{\|c\|_\infty} V(t) \triangleq -\mu V(t) \tag{2.18}$$

From the inequality (2.18), it can be easily concluded that

$$V(t) \le e^{-\mu(t-t_0)} V(t_0) \tag{2.19}$$

i.e.

$$|s(t)| \le e^{-\frac{1}{2}\mu(t-t_0)} |s(t_0)| \tag{2.20}$$

Therefore, (2.20) implies that $s(t)$ converges to zero exponentially.

In order to prove that the state approaches to zero, the next well known lemma is cited [1].

Lemma 2.1 For the stable matrix Γ, there exist positive constants d_1 and d_2, such that

$$\|\exp(\Gamma t)\|_1 \le d_2 \cdot e^{-d_1 t} \tag{2.21}$$

Now, let $\underline{x} = [x_1, x_2, \cdots, x_{n-1}]^T$. Regarding to the definition of $s(t)$ and the relation $\dot{x}_i(t) = x_{i+1}(t)$ for $i = 1, 2, \cdots, n-1$, we get

$$\dot{\underline{x}}(t) = \Gamma \underline{x}(t) + [0, \cdots, 0, 1]^T s(t) \tag{2.22}$$

Integrating equation (2.22) yields

$$\underline{x}(t) = \exp(\Gamma(t-t_0))\underline{x}(t_0) + \int_{t_0}^{t} \exp(\Gamma(t-\tau))[0, \cdots, 0, 1]^T s(\tau) d\tau \tag{2.23}$$

Then, taking the norm on (2.23) yields

$$\|\underline{x}(t)\|_1 \le d_2 e^{-d_1(t-t_0)} \|\underline{x}(t_0)\|_1 + d_2 \int_{t_0}^{t} e^{-d_1(t-\tau)} e^{-\frac{1}{2}\mu(\tau-t_0)} |s(t_0)| d\tau \tag{2.24}$$

where Lemma 2.1 is used. From (2.24), it can be easily concluded that $\underline{x}(t)$ approaches to zero exponentially. By the fact $x_n(t) = s(t) - \underline{c} \cdot \underline{x}(t)$, we get $x_n(t) \to 0$. Therefore, we have proved that $x(t) \to 0$ (as $t \to \infty$).

2.3 Computer-Controlled Continuous-Time Variable Structure Systems

2.3.1 Mathematical Preliminaries

From Assumption 2.2, i.e. $\alpha_i \le a_i \le \beta_i$ (for $1 \le i \le n$), the following inequality can be obtained.

$$-\frac{\beta_i - \alpha_i}{2} \le a_i - \frac{\alpha_i + \beta_i}{2} \le \frac{\beta_i - \alpha_i}{2} \tag{2.25}$$

So, the matrix A can be decomposed as

$$A = \begin{bmatrix} 0 & 1 & 0 & \cdots & 0 \\ 0 & 0 & 1 & \cdots & 0 \\ \cdot & \cdot & \cdot & \cdots & \cdot \\ 0 & 0 & 0 & \cdots & 1 \\ -p_1 & -p_2 & -p_3 & \cdots & -p_n \end{bmatrix} + \begin{bmatrix} 0 & 0 & 0 & \cdots & 0 \\ 0 & 0 & 0 & \cdots & 0 \\ \cdot & \cdot & \cdot & \cdots & \cdot \\ 0 & 0 & 0 & \cdots & 0 \\ -q_1 & -q_2 & -q_3 & \cdots & -q_n \end{bmatrix} \triangleq P + Q \tag{2.26}$$

where

$$p_i = a_i - \frac{\alpha_i + \beta_i}{2}, \quad q_i = \frac{\alpha_i + \beta_i}{2}, \quad (\text{for } 1 \le i \le n) \tag{2.27}$$

In this paper, we denote

$$\gamma_i = \frac{\beta_i - \alpha_i}{2} \ (1 \le i \le n), \quad m_1 = \max_{i=1}^{n}\{\gamma_i\}, \quad m_2 = \max_{i=1}^{n}\{|q_i|\} \tag{2.28}$$

Because α_i and β_i $(1 \le i \le n)$ are known by Assumption 2.2, the above quantities are also known.

The following lemma gives the upper bounds of $\|P\|_1$ and $\|A\|_1$.

Lemma 2.2 The upper bounds of $\|P\|_1$ and $\|A\|_1$ can be estimated as

$$\|P\|_1 \le 1 + m_1, \quad \|A\|_1 \le 1 + m_1 + m_2 \tag{2.29}$$

Proof: By the definition of $\|\cdot\|_1$ in (2.8), it is easy to see that

$$\|P\|_1 = 1 + \max_{i=1}^{n}\{|p_i|\} \le 1 + \max_{i=1}^{n}\{\gamma_i\} = 1 + m_1, \quad \|Q\|_1 = \max_{i=1}^{n}\{|q_i|\} = m_2$$

Thus, the lemma is obvious.

2.3.2 Decision of the Piece-Wise Constant Input

When the system is controlled by a digital computer, the continuous-time control law (2.13) can not be realized. So, the implementation problem of the control law (2.13) must be discussed. In this paper, the zero-order-hold of the input (2.13) will be used to control the system.

Let $x(k)$ denote the value of the state $x(t)$ at time kh, where h is the sampling period. The instantaneous value $u(k)$ of the continuous-time control (2.13) at time kh is used as the piece-wise constant input on the interval $[kh, (k+1)h)$, i.e.

$$u(k) = -c_1 x_2(k) - \cdots - c_{n-1} x_n(k) - \sum_{i=1}^{n} (\psi_i(k) + \delta) \cdot x_i(k) \cdot \mathrm{sgn}(x_i(k) \cdot s(k)) \quad (2.30)$$

where $\psi_i(k) = \begin{cases} -\alpha_i, & x_i(k)s(k) > 0 \\ \beta_i, & x_i(k)s(k) < 0 \end{cases}$, δ is a positive constant.

The above control input can also be rewritten as

$$\begin{aligned} u(k) &= -\sum_{i=1}^{n-1} c_i x_{i+1}(k) + \sum_{i=1}^{n} q_i x_i(k) - \sum_{i=1}^{n} \{(\psi_i(k) + \delta)\,\mathrm{sgn}(x_i(k)s(k)) + q_i\} x_i(k) \\ &= -\sum_{i=1}^{n-1} c_i x_{i+1}(k) + \sum_{i=1}^{n} q_i x_i(k) - \begin{cases} \sum_{i=1}^{n} (-\alpha_i + \delta + q_i) x_i(k) \ as\ x_i(k)s(k) > 0 \\ \sum_{i=1}^{n} (-(\beta_i + \delta) + q_i) x_i(k) as\, x_i(k)s(k) < 0 \end{cases} \\ &= -\sum_{i=1}^{n-1} c_i x_{i+1}(k) + \sum_{i=1}^{n} q_i x_i(k) - \sum_{i=1}^{n} (\gamma_i + \delta) x_i(k)\,\mathrm{sgn}(x_i(k)s(k)) \end{aligned} \quad (2.31)$$

The block diagram of the computer-controlled continuous-time variable structure systems with sliding modes is shown in Figure 2.1, where $abs(x(t))$ is defined as $abs(x(t)) \triangleq [|x_1(t)|, \cdots, |x_n(t)|]^T$.

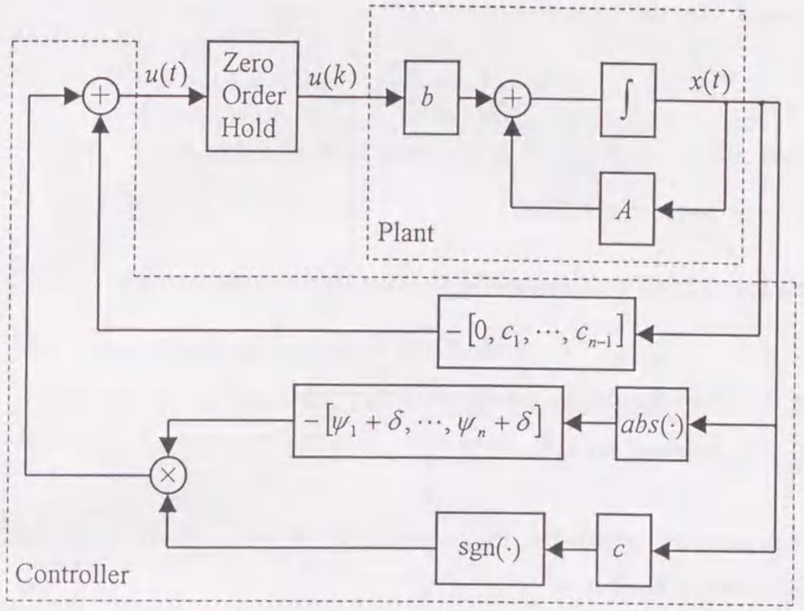

Fig. 2.1 The block diagram of the computer-controlled continuous-time variable structure systems with sliding modes

2.3.3 Occurrence of the Weak-Pseudo-Sliding Mode

With the piece-wise control input $u(k)$ on the interval $[kh, (k+1)h)$, the system on this interval will be described by

$$\dot{x}(t) = Ax(t) + bu(k) \quad (2.32)$$

Solving the above equation on the interval $[kh, (k+1)h)$ yields

$$x(t) = \exp\{A(t-kh)\}x(k) + \int_{kh}^{t} \exp\{A(t-\tau)\}d\tau \cdot b \cdot u(k) \quad (2.33)$$

Now, let $t = (k+1)h$, the following discrete-time system is obtained.

$$x(k+1) = \exp(Ah)x(k) + \int_{0}^{h} \exp\{A\tau\}d\tau \cdot b \cdot u(k) \quad (2.34)$$

First of all, the controllability of the discrete-time system (2.34) must be investigated. For this purpose, the following two results are cited.

Lemma 2.3 The discrete-time system (2.34) is controllable if and only if

$$\mathrm{Im}(\lambda_i - \lambda_j) \neq \frac{2n\pi}{h}, \quad n = \pm 1, \pm 2, \cdots \tag{2.35}$$

whenever $\mathrm{Re}(\lambda_i - \lambda_j) = 0$, λ_i are the eigenvalues of matrix A.

Proof: For the proof, see [39].

Lemma 2.4 For any matrix norm $\|\cdot\|$, the following inequality is valid.

$$|\lambda_i(B)| \leq \|B\| \tag{2.36}$$

where $\lambda_i(B)$ are the eigenvalues of matrix B.

Proof: For the proof, see [19].

Upon the above preparation, the controllability of system (2.34) can be clarified by the following Theorem.

Theorem 2.1 If the sampling period h is chosen as

$$h \leq \frac{\pi}{2(1 + m_1 + m_2)} \tag{2.37}$$

then the discrete-time system (2.34) is controllable.

Proof: From Lemma 2.4,

$$\left|\mathrm{Im}(\lambda_i - \lambda_j)\right| \leq 2\|A\|_1$$

Thus, by applying Lemma 2.2 and Lemma 2.3, the theorem is obvious.

Now, a difference equation of $s(k)$ will be derived from (2.34). Thus, pre-multiplying (2.34) by c yields

$$\begin{aligned} s(k+1) &= c \cdot \exp(Ah)x(k) + c\int_0^h \exp\{A\tau\}d\tau \cdot b \cdot u(k) \\ &= s(k) + c\{\exp(Ah) - I\}x(k) + c\int_0^h \exp\{A\tau\}d\tau \cdot b \cdot u(k) \\ &= s(k) + c\int_0^h \exp\{A\tau\}d\tau\{Ax(k) + b \cdot u(k)\} \end{aligned} \tag{2.38}$$

Substituting the expression (2.31) of $u(k)$ into (2.38) gives

$$\begin{aligned} s(k+1) &= s(k) + c\int_0^h \exp(A\tau)d\tau\{A + b \cdot [q_1, -c_1 + q_2, \cdots, -c_{n-1} + q_n]\}x(k) \\ &\quad - c\int_0^h \exp(A\tau)d\tau \cdot b \cdot \sum_{i=1}^{n}(\gamma_i + \delta)x_i(k)\,\mathrm{sgn}\{x_i(k)s(k)\} \\ &= s(k) + c\int_0^h \exp(A\tau)d\tau\{P - b[0, c_1, \cdots, c_{n-1}]\}x(k) \\ &\quad - c\int_0^h \exp(A\tau)d\tau \cdot b\sum_{i=1}^{n}(\gamma_i + \delta)|x_i(k)|\,\mathrm{sgn}(s(k)) \end{aligned} \tag{2.39}$$

By some simple calculations, we have

$$c \cdot \{P - b \cdot [0, c_1, \cdots, c_{n-1}]\} = -[p_1, \cdots, p_n] \tag{2.40}$$

$$c \cdot b = 1 \tag{2.41}$$

Thus, substituting (2.40) and (2.41) into (2.39) yields

$$\begin{aligned} s(k+1) &= s(k) - h[p_1, \cdots, p_n]x(k) \\ &\quad + c\int_0^h \{\exp(A\tau) - I\}d\tau\{P - b \cdot [0, c_1, \cdots, c_{n-1}]\}x(k) \\ &\quad - h\sum_{i=1}^{n}\gamma_i|x_i(k)|\,\mathrm{sgn}(s(k)) - h\delta\sum_{i=1}^{n}|x_i(k)|\,\mathrm{sgn}(s(k)) \\ &\quad + c\int_0^h \{\exp(A\tau) - I\}d\tau \cdot b\sum_{i=1}^{n}(\gamma_i + \delta)|x_i(k)|\,\mathrm{sgn}(s(k)) \\ &= s(k) - h[p_1, \cdots, p_n]x(k) \\ &\quad + \frac{1}{2}h^2 c \cdot \exp(Ah\theta)A\{P - b \cdot [0, c_1, \cdots, c_{n-1}]\}x(k) \\ &\quad - h\sum_{i=1}^{n}\gamma_i|x_i(k)|\,\mathrm{sgn}(s(k)) - h\delta\sum_{i=1}^{n}|x_i(k)|\,\mathrm{sgn}(s(k)) \\ &\quad + \frac{1}{2}h^2 c \cdot \exp(Ah\theta)Ab\sum_{i=1}^{n}(\gamma_i + \delta)|x_i(k)|\,\mathrm{sgn}(s(k)) \end{aligned} \tag{2.42}$$

where the fact that there exists a constant θ $(0 < \theta < 1)$ such that

$$\int_0^h \{\exp(A\tau) - I\}d\tau = \frac{1}{2}A^2h^2\exp(Ah\theta) \tag{2.43}$$

is used.

In order to simplify (2.42), we denote

$$F(h,x(k)) \triangleq \left\{-[p_1,\cdots,p_n]+\frac{1}{2}h\cdot c\cdot\exp(Ah\theta)A\{P-b\cdot[0,c_1,\cdots,c_{n-1}]\}\right\}x(k)$$

$$+\frac{1}{2}h\cdot c\cdot\exp(Ah\theta)Ab\sum_{i=1}^{n}(\gamma_i+\delta)|x_i(k)|\operatorname{sgn}(s(k)) \tag{2.44}$$

$$G(x(k)) \triangleq \sum_{i=1}^{n}\gamma_i|x_i(k)|+\delta\sum_{i=1}^{n}|x_i(k)| \tag{2.45}$$

Consequently, (2.43) can be written in the next compact form.

$$s(k+1)=s(k)+hF(h,x(k))-hG(x(k))\operatorname{sgn}(s(k)) \tag{2.46}$$

The above difference equation of hyperplane $s(k)$ will be used to derive the conditions of the occurrence of the weak-pseudo-sliding-mode behavior. For this purpose, first of all, the upper bound of $\|\exp(Ah\theta)\|_1$ will be estimated.

Lemma 2.5 If h meets the condition

$$h\le\frac{\ln\frac{3}{2}}{1+m_1+m_2} \tag{2.47}$$

then

$$\|\exp(Ah\theta)\|_1<\frac{3}{2} \tag{2.48}$$

Proof: Observe that

$$\|\exp(Ah\theta)\|_1\le\exp(h\theta\|A\|_1)\le\exp(h\theta(1+m_1+m_2))$$

Therefore, by using the fact $0<\theta<1$, this lemma can be proved.

Now, some estimations of the quantities $F(h,x(k))$ and $G(x(k))$ will be made in the following two lemmas.

Lemma 2.6 If h is chosen as

$$h\le\min\left\{\frac{\ln\frac{3}{2}}{1+m_1+m_2},\ \frac{7\delta}{6\|c\|_1(1+m_1+m_2)(1+2m_1+\|c\|_1+\delta)}\right\} \tag{2.49}$$

then

$$\left|\frac{1}{2}h\cdot c\cdot\exp(Ah\theta)A\{P-b\cdot[0,c_1,\cdots,c_{n-1}]\}x(k)\right|$$

$$+\left|\frac{1}{2}h\cdot c\cdot\exp(Ah\theta)Ab\sum_{i=1}^{n}(\gamma_i+\delta)|x_i(k)|\operatorname{sgn}(s(k))\right|$$

$$<\frac{7}{8}\delta\|x(k)\|_1 \tag{2.50}$$

Proof: If h meets (2.49), then

$$\left|\frac{1}{2}h\cdot c\cdot\exp(Ah\theta)A\{P-b\cdot[0,c_1,\cdots,c_{n-1}]\}x(k)\right|$$

$$+\left|\frac{1}{2}h\cdot c\cdot\exp(Ah\theta)Ab\sum_{i=1}^{n}(\gamma_i+\delta)|x_i(k)|\right|$$

$$\le\frac{1}{2}h\cdot\|c\|_1\cdot\|\exp(Ah\theta)\|_1\cdot\|A\|_1\{(\|P\|_1+\|c\|_1)+(m_1+\delta)\}\|x(k)\|_1$$

$$<\frac{3}{4}h\|c\|_1(1+m_1+m_2)(1+2m_1+\|c\|_1+\delta)\|x(k)\|_1 \tag{2.51}$$

where Lemma 2.2 and Lemma 2.5 are used. By (2.51), this lemma can be easily verified.

Lemma 2.7 If the sampling period h meets the following condition

$$h\le\min\left\{\frac{\ln\frac{3}{2}}{1+m_1+m_2},\ \frac{7\delta}{6\|c\|_1(1+m_1+m_2)(1+2m_1+\|c\|_1+\delta)},\ \frac{\varepsilon}{2(m_1+\delta)}\right\} \tag{2.52}$$

then

$$\frac{\delta\|x(k)\|_1}{8}+|F(h,x(k))|<G(x(k))\le\frac{\varepsilon\|x(k)\|_1}{2h} \tag{2.53}$$

Proof: From the definition of $F(h,x(k))$ in (2.44), applying Lemma 2.6, we have

$$|F(h,x(k))|<\sum_{i=1}^{n}|p_ix_i(k)|+\frac{7}{8}\delta\|x(k)\|_1$$

$$\le\sum_{i=1}^{n}\gamma_i|x_i(k)|+\frac{7}{8}\delta\|x(k)\|_1 \tag{2.54}$$

So,

$$\frac{\delta\|x(k)\|_1}{8} + |F(h,x(k))| < \sum_{i=1}^{n}\gamma_i|x_i(k)| + \delta\|x(k)\|_1 = G(x(k)) \qquad (2.55)$$

On the other hand, from the definition of $G(x(k))$ in (2.45), it is easily to know that

$$G(x(k)) \le (m_1 + \delta)\|x(k)\|_1 \qquad (2.56)$$

Thus, if h is chosen as $h \le \dfrac{\varepsilon}{2(m_1+\delta)}$, the next relation is obvious.

$$G(x(k)) \le \frac{\varepsilon\|x(k)\|_1}{2h} \qquad (2.57)$$

Therefore, by combining (2.55) and (2.57), this lemma can be proved.

For simplicity, we define

$$h_m \triangleq \min\left\{\frac{\ln\frac{3}{2}}{1+m_1+m_2}, \frac{7\delta}{6\|c\|_1(1+m_1+m_2)(1+2m_1+\|c\|_1+\delta)}, \frac{\varepsilon}{2(m_1+\delta)}\right\} \qquad (2.58)$$

Lemma 2.7 implies that if $h \le h_m$, then the sign of the term $F(h,x(k)) - G(x(k))\mathrm{sgn}(s(k))$ in (2.46) is governed by $s(k)$. This result will be used in the estimation of $s(k+1)$.

Summing up the above lemmas, we obtain the following theorem.

Theorem 2.2 For the system (2.32) with the input (2.30), if the sampling period h satisfies $h \le h_m$, then either a weak-pseudo-sliding mode takes place along the hyperplane $s(k) = 0$ or $s(k)$ is monotonically decreasing and

$$x(k) \to 0 \quad \text{and} \quad s(k) \to 0 \quad (\text{as } k \to \infty) \qquad (2.59)$$

Proof: The proof is given in the Appendix.

In order to guarantee the occurrence of the weak-pseudo-sliding mode behavior, the upper bound of the sampling period depends on not only the known bounds of the

parameters, the choice of the sliding hyperplane and the positive constant δ in the control input, but also the value of ε.

2.3.4 Stability of the Controlled System by Zero-Order-Hold Input

By Theorem 2.2, if h is chosen as $h \le h_m$, we only need to investigate the stability of the control system whose discretized system results in a weak-pseudo-sliding mode. It might be argued that if ε is chosen to be small enough, the weak-pseudo-sliding mode may result in a stable behavior.

To begin with, the next lemma is given to illustrate the connection between the hyperplane at every instant in $k_{i+1}h \ge t \ge k_i h$ and the state at instant $k_i h$.

Lemma 2.8 If h is chosen as (2.49), we can also get

$$|s(t)| < \varepsilon\|x(k_i)\|_1, \text{ for } k_{i+1}h \ge t \ge k_i h \qquad (2.60)$$

Proof: The proof is given in the Appendix.

In order to study the stability behavior, we start with the next equation.

$$\dot{\underline{x}}(t) = \Gamma\underline{x}(t) + [0,\cdots,0,1]^T s(t) \qquad (2.61)$$

Denote

$$L = \left[\frac{1}{hd_1}\ln 8d_2\right] + 1 \qquad (2.62)$$

where $[\rho]$ represents the integer part of ρ. By applying Lemma 2.1, it is obvious that

$$\|\exp(\Gamma Lh)\|_1 \le d_2 e^{-d_1 Lh} \le \frac{1}{8} \qquad (2.63)$$

Now, discretizing the differential equation (2.22) by L steps yields

$$\underline{x}(k+L) = \exp(\Gamma Lh)\underline{x}(k) + \int_0^{Lh}\exp\{\Gamma(Lh-\tau)\}[0,\cdots,0,1]^T s(kh+\tau)d\tau \qquad (2.64)$$

Thus, taking the norm on the both sides of (2.63) gives

$$\|\underline{x}(k+L)\|_1 \le \|\exp(\Gamma Lh)\|_1 \|\underline{x}(k)\|_1 + \int_0^{Lh} \|\exp(\Gamma(Lh-\tau))\|_1 |s(kh+\tau)| d\tau$$

$$\le \frac{1}{8}\|\underline{x}(k)\|_1 + \int_0^{Lh} d_2 e^{-d_1(Lh-\tau)} |s(kh+\tau)| d\tau \tag{2.65}$$

For simplicity, we define

$$\varepsilon_m \triangleq \frac{3d_1}{3d_1 + 4d_2(1+\|\underline{c}\|_\infty)} \tag{2.66}$$

Lemma 2.9 If h and ε are chosen as $h \le h_m$ and $\varepsilon \le \varepsilon_m$ respectively, then there exists a subsequence $\{k_{i_j}\}$, $j = 1,2,3,\cdots$, which satisfies $k_{i_{j+1}} \ge k_{i_j} + L$, such that

$$\|\underline{x}(k_{i_j} + L + \ell)\|_1 \le \frac{7}{8} \max_{l=0}^{L-1} \{\|\underline{x}(k_{i_j} + l)\|_1\} \tag{2.67}$$

for $0 \le \ell \le k_{i_{j+1}} - k_{i_j} - 1$.

Proof: The proof is given in the Appendix.

Summing up the above results, we obtain the central theorem of this chapter.

Theorem 2.3 For the system (2.32) with the input (2.30), if the sampling period h and ε are chosen as $h \le h_m$ and $\varepsilon \le \varepsilon_m$ respectively, then $s(t) \to 0$ and $x(t) \to 0$ (as $t \to \infty$).

Proof: By the result of Lemma 2.9,

$$\|\underline{x}(k_{i_{j+1}} + l)\|_1 \le \frac{7}{8} \max_{l=0}^{L-1} \{\|\underline{x}(k_{i_j} + l)\|_1\} \tag{2.68}$$

for $0 \le l \le L-1$. Thus, it is easy to know that

$$\max_{l=0}^{L-1} \{\|\underline{x}(k_{i_j} + l)\|_1\} \to 0, \text{ as } j \to \infty \tag{2.69}$$

Therefore, by (2.67), we can concluded that $\underline{x}(k) \to 0$ as $k \to \infty$. Then, from (A.24), it is easy to see that $x(k) \to 0$ as $k \to \infty$. By applying Lemma 2.8, we have $s(t) \to 0$ $(t \to \infty)$. As it is proved in the second section of this chapter, based on (2.22), we can prove that $\underline{x}(t) \to 0$ $(t \to \infty)$. Therefore, from the fact

$x_n(t) = s(t) - \underline{c} \cdot \underline{x}(t)$, we have $x_n(t) \to 0$ as $t \to \infty$. Consequently, $x(t) \to 0$ as $t \to \infty$.

It can be seen that the quantity ε_m only depends on the selection of the hyperplane. The estimated upper bound h_m of the sampling period depends on not only the selection of the hyperplane and the constant δ in the control input, but also the known upper and lower bounds of the unknown parameters. It can be seen that h_m is reciprocal to the difference of the upper and lower bounds of the unknown parameters. It should be point out that Theorem 2.3 only gives a sufficient condition for the sampled data system to be stable by employing the zero-order-hold of the continuous-time VSS controller without any modification.

To summary the algorithm in this chapter, Table 2.1 is presented.

Table 2.1 The algorithm of the computer controlled continuous-time variable structure systems with sliding modes

Plant	$\dot{x}(t) = Ax(t) + bu(t)$
Sampling period	$h \le h_m$
Piece-wise constant input	$u(k) = -c_1 x_2(k) - \cdots - c_{n-1} x_n(k) - \sum_{i=1}^{n} (\psi_i(k) + \delta) \cdot x_i(k) \cdot \text{sgn}(x_i(k) \cdot s(k))$

2.4 Simulation Results

Consider the two-dimensional system described by

$$\dot{x}(t) = \begin{bmatrix} 0 & 1 \\ 0.15 & 3 \end{bmatrix} x(t) + \begin{bmatrix} 0 \\ 1 \end{bmatrix} u(t) \tag{2.70}$$

where $a_1 = -0.15$, $a_2 = -3$. Here the genuine values of $a_i (i = 1,2)$ are unknown,

but their upper and lower bounds $\alpha_i, \beta_i (\alpha_i \le a_i \le \beta_i, i = 1,2)$ are known as

$$\alpha_1 = -0.5, \beta_1 = 0.5, \alpha_2 = -3.5, \beta_2 = -2.5 \tag{2.71}$$

Thus, we have $m_1 = 0.5$, $m_2 = 3$.

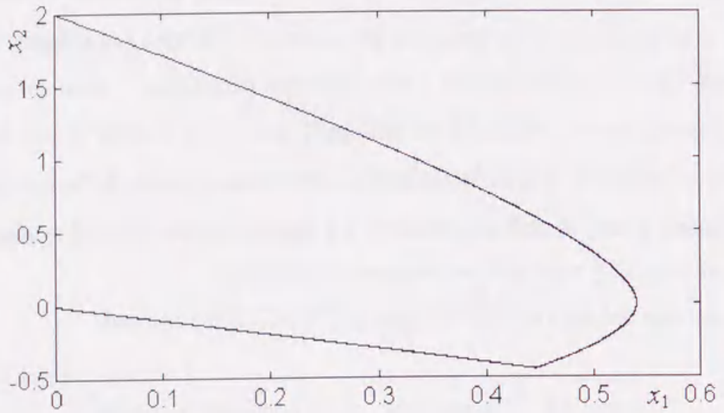

Fig. 2.2 A continuous-time sliding mode where the continuous control input (2.13) is used.

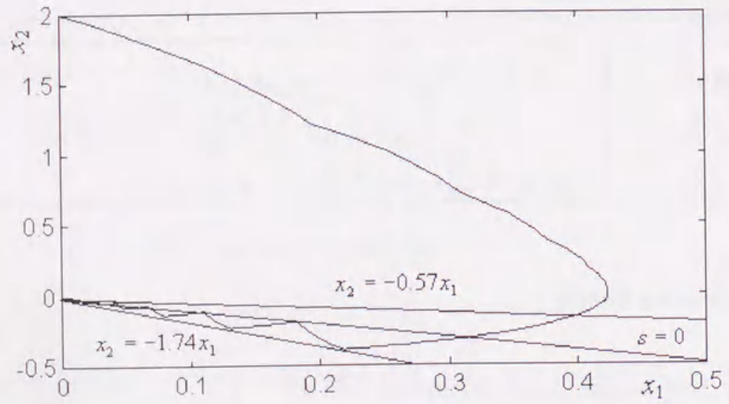

Fig. 2.3 A stable weak-pseudo-sliding mode with the sampling period $h = 0.08 = h_m$.

Now, we choose

$$c = [1, 1], \quad \delta = 1.3 \tag{2.72}$$

So, d_1 and d_2 in Lemma 2.1 can be chosen as $d_1 = 1$ and $d_2 = 1$. Therefore, the values of ε_m and h_m can be calculated as

$$\varepsilon_m = 0.27 \ , \ h_m = 0.08 \tag{2.73}$$

Thus, the sector field $|s(k_i)| < \varepsilon \|x(k_i)\|_1$ defined in Definition 2.3 can be calculated as

$$-1.74x_1(k_i) < x_2(k_i) < -0.57x_1(k_i) \quad \text{as} \quad x_1(k_i) > 0 \tag{2.74}$$

$$-1.74x_1(k_i) > x_2(k_i) > -0.57x_1(k_i) \quad \text{as} \quad x_1(k_i) < 0 \tag{2.75}$$

In the practical simulation process, the orbit starting at $x_0 = [0, 2]^T$ is investigated. Figure 2.2 illustrates a continuous-time sliding mode where the continuous control input (2.13) is used. Figure 2.3 illustrates a stable weak-pseudo-sliding mode with the sampling period $h = 0.08 = h_m$.

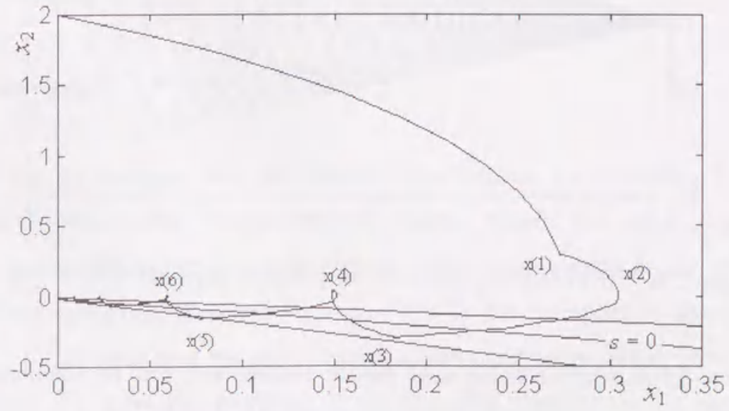

Fig. 2.4 A stable weak-pseudo-sliding mode with the sampling period $h = 0.11 > h_m$

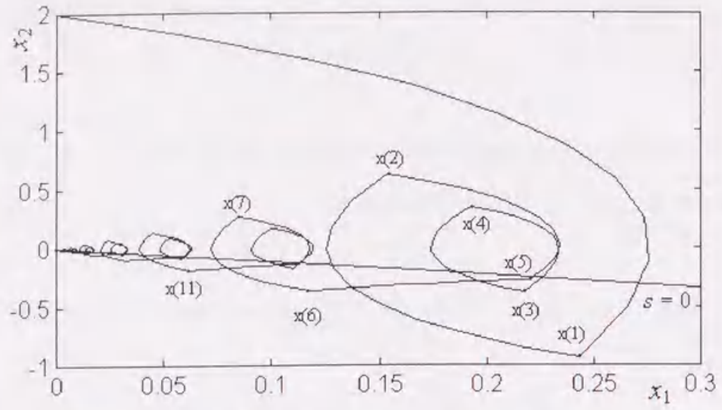

Fig. 2.5 A stable weak-pseudo-sliding mode with the sampling period $h = 0.16 > h_m$.

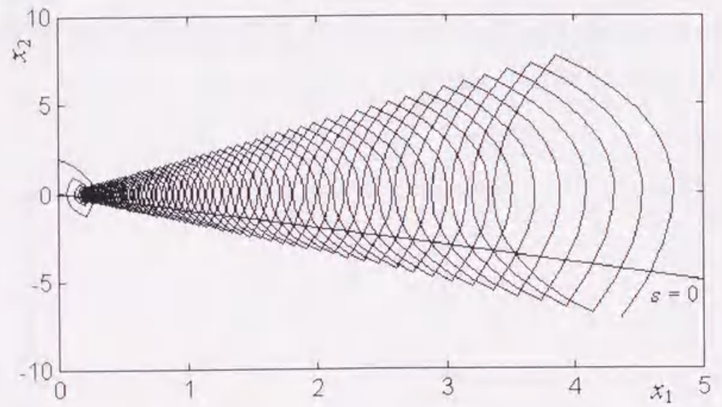

Fig. 2.6 An unstable system with the sampling period $h = 0.17 > h_m$.

Figure 2.4 illustrates a stable weak-pseudo-sliding mode with the sampling period $h = 0.11 > h_m$. Corresponding to Definition 2.3, it can be seen that $k_i = 2i + 1$ for $i = 1, 2, \cdots$. It is obvious that this kind of sliding mode can not be precisely described by the traditional definitions of the discrete-time sliding mode behavior.

Figure 2.5 illustrates a stable system with the sampling period $h = 0.16 > h_m$. From Definition 2.3, the behavior of this system can not be regarded as weak-pseudo-sliding mode if the sector defined by (2.74) and (2.75) is considered. But if the sector is chosen to be a little wider (for example, when ε is chosen as $\varepsilon = 0.4$, the sector is defined as $-\frac{3}{7}x_1(k_i) < x_2(k_i) < -\frac{7}{3}x_1(k_i)$ while $x_1(k_i) < 0$; $-\frac{3}{7}x_1(k_i) > x_2(k_i) > -\frac{7}{3}x_1(k_i)$ while $x_1(k_i) > 0$), the behavior of this system can be regarded as weak-pseudo-sliding mode (where $k_i = \begin{cases} 3+5j & \text{if } i = 3j+1 \\ 5+5j & \text{if } i = 3j+2 \\ 6+5j & \text{if } i = 3j+3 \end{cases}$, for $j = 0, 1, 2, \cdots$). This is because $\varepsilon_m = 0.27$ is only one of the sufficient conditions for the system to be stable.

Figure 2.6 illustrates an unstable system with the sampling period $h = 0.17 > h_m$.

Since Theorem 2.3 only gives a sufficient condition for the systems to be stable, Figures 2.4 and 2.5 do not contradict with Theorem 2.3. Figure 2.6 tells us that, if the sampling period is chosen to be too large, the sampled data system will result in an unstable system.

2.5 Conclusions

For solving the problem associated with implementation by computer of a well designed continuous-time variable structure control system, this paper proposes a more general definition, which is called "discrete-time weak-pseudo-sliding mode", to describe the zigzag behavior along the hyperplane for the corresponding discrete-time system. An estimation of the upper bound of the sampling period is presented to ensure that the weak-pseudo-sliding mode can take place along the prescribed hyperplane. If the chosen sampling period is not greater than this upper bound, the zero-order-hold of the continuous-time VSC structure can still be used without any modification, and the stability of the sampled data system can also be guaranteed.

Computer simulations have shown the effectiveness and practicality of the proposed algorithm.

For the multivariable uncertain systems, the upper bound of the sampling period to assure the stability of the sampled-data systems is expected to be derived.

Chapter 3

Robust Adaptive Quasi-Sliding Mode Controller for Discrete-Time Systems

3.1 Introduction

Sliding mode control of continuous-time systems has been intensively studied in the past 30 years [57,71]. It is well known this method offers excellent robustness and invariance properties to uncertainties. But, discrete-time sliding mode control has received attention only recently [2,14,18,38,42,49,71]. The important difference between the continuous-time and discrete-time sliding mode control is that the latter may not be robust with respect to uncertainties, if the design philosophies for continuous-time systems are extended to the discrete-time systems. Unless special modifications are taken, the existence of sliding mode can not be guaranteed in the presence of uncertainties.

In order to present the main characteristics of the discrete sliding mode behavior, consider the following system

$$x(k+1) = Ax(k) + bu(k) + f(k) \tag{3.1}$$

where $x \in R^n$, $u \in R^1$, $f \in R^n$ represent the state, control and system uncertainty respectively, and (A,b) is a known controllable pair. Define

$$s(k) = Gx(k), \tag{3.2}$$

where $G^T \in R^n$ is chosen such that $Gb \neq 0$. The ideal sliding surface is defined by

$$Gx(k) = 0. \tag{3.3}$$

The so called "equivalent control" $u_{eq}(k)$ may be derived by letting [71]

$$s(k+1) = Gx(k+1) = GAx(k) + Gbu(k) + Gf(k) = 0. \tag{3.4}$$

Thus, the "equivalent control" $u_{eq}(k)$ can be defined by

$$u_{eq}(k) = -(Gb)^{-1}\{GAx(k) + Gf(k)\}. \tag{3.5}$$

The ideal sliding motion is then described by

$$x(k+1) = (I - b(Gb)^{-1}G)\{Ax(k) + f(k)\}. \tag{3.6}$$

The above equation also describes the "equivalent system motion". If $f(k)$ is matched, i.e.

$$f(k) = b \cdot \bar{f}(k), \tag{3.7}$$

then, Equation (3.6) becomes

$$x(k+1) = A_{eq}x(k) \triangleq (I - b(Gb)^{-1}G)Ax(k). \tag{3.8}$$

Note that this motion is independent of the matched uncertainties and the actual values of the control $u(k)$ during the sliding mode and depends only on the choice of G. This is the well-known "invariance" property of the sliding mode. The equation $s(k) = 0$ enables the reduction of the system order, and the desired dynamics of the sliding mode, governed by the $(n-1)$-th order system, can be designed by appropriate choice of the vector G (which is usually chosen such that A_{eq} is a stable matrix) in the sliding mode Equation (3.8). Thus, the controlled system can be stabilized by choosing the control to drive the state into the sliding surface.

It is obvious that the linear pole placement state feedback control $u(k) = -(Gb)^{-1}GAx(k)$ can stabilize the nominal system of (3.1). But this control can not work well in the presence of uncertainties. Corresponding to different types of the uncertainty $f(k)$, different robust controllers are proposed to drive the state into the sliding surface [2,14,15,38,42,49].

A typical robust switching controller is proposed in [18] for $f(k) = bdx(k)$, where the entries of $d = [d_1, d_2, \cdots, d_n]$ is bounded by a known constant $\bar{d}$. In the region near the sliding surface $|s(k)| \leq \varepsilon \sum_{i=1}^{n} |x_i(k)|$, the linear state feedback control (the equivalent control component of the nominal system) is used. Outside of this region, feedback coefficients are changed. By using this control, the quantity $s(k)$ asymptotically approaches to zero. But, in the proposed switching controller, the upper bound $\bar{d}$ need to be small and known, which may not be satisfied.

If the unknown term $f(k)$ is matched and slow varying with respect to k, switching and nonswitching controllers are proposed in [2] and [14], respectively. The quantity $s(k)$ can be controlled to approach to zero asymptotically if $|f(k) - f(k-1)| \leq \eta |f(k-1)|$, where $\eta \geq 0$ is known [14]. It is clear that the above assumption may not be easy to satisfy. To overcome this difficulty, [2] proposes a nonswitching sliding mode controller, which contains the estimation of the unknown term $f(k)$, to guarantee the bounded motion of the state about the sliding surface. The controller proposed in [2] is simple and easy to be implemented.

In the presence of bounded uncertainties $f(k)$, it is almost impossible to control the state to approach to zero by just using the upper and lower bounds of $f(k)$ even though $f(k)$ is matched [14,22,71]. Instead of controlling the state to approach to zero, bounded motion about the sliding surface can be guaranteed by just employing the equivalent control component of the nominal system (a linear state feedback), where only the boundedness of $f(k)$ is required [38,49].

As the concept "discrete-time sliding mode" is differently defined in [2,14,18,38, 42,49,71], it needs to be clarified [Chapter 2 of this thesis, 71]. In this paper, "discrete sliding mode" means that the sliding surface $s(k) = 0$ is reached in a finite time and continues to remain on it thereafter, whereas "discrete quasi-sliding mode" refers to the asymptotic approaching of $s(k)$ to zero.

This chapter deals with the quasi-sliding mode control problem for the discrete-time systems with model uncertainties, unmodeled dynamics and bounded disturbances. The proposed method is adaptive control in conjunction with a sliding mode based controller design. Section 3.2 gives the problem formulation. In section 3.3, first, adaptive algorithms with the dead-zones are formulated even though the upper and lower bounds of the disturbance are unknown. Then, based on the estimates of the unknown parameters, a controller is proposed to guarantee the existence of the quasi-sliding mode about the sliding surface. In section 3.4, simulation results are presented to illustrate the proposed algorithm.

3.2 Problem Formulation

Consider the discrete-time system described by

$$x(k+1) = Ax(k) + bu(k) + f(k,u(k),x(k)), \tag{3.9}$$

where *x(k)* is an $n\times 1$ state vector, *u(k)* is a scalar input, $f(k,u(k),x(k))$ is an $n\times 1$ uncertain vector; A and b are known matrices of appropriate dimensions.

Assumption 3.1 The state $x(k)$ is available.

Assumption 3.2 (A, b) is a controllable pair.

In this paper, the norm $\|\cdot\|_2$ is defined as

$$\|x(k)\|_2 = \sqrt{\sum_{i=1}^{n}(x_i(k))^2} \tag{3.10}$$

for the vector $x(k) = [x_1(k),\cdots,x_n(k)]^T$.

For the uncertainty $f(k,u(k),x(k))$, we make the following assumptions.

Assumption 3.3 The uncertainty $f(k,u(k),x(k))$ is of the following form

$$f(k,u(k),x(k)) = h_0(u(k),x(k)) + h_1(k,u(k),x(k)) + h_2(k), \tag{3.11}$$

where

$$\begin{aligned} h_0(u(k),x(k)) &= bdx(k) + \delta bu(k) \\ &\triangleq b[d_1,\cdots,d_n]x(k) + \delta bu(k), \end{aligned} \tag{3.12}$$

$\|h_1(k,u(k),x(k))\|_2$ and $\|h_2(k)\|_2$ are bounded by

$$\|h_1(k,u(k),x(k)\|_2 \le \alpha\{\|x(k)\|_2 + |u(k)|\} \tag{3.13}$$

and

$$\|h_2(k)\|_2 \le \nu, \tag{3.14}$$

respectively, i.e. $f(k,u(k),x(k))$ is composed of matched and unmatched uncertainties.

Assumption 3.4 $d_i (i=1,\cdots,n)$ and δ are unknown constants; α is a known positive constant which is very small; ν is an unknown positive constant.

Assumption 3.5 There exists a known constant δ_m satisfying $|\delta_m| \le |1+\delta|$ and $(1+\delta)\delta_m > 0$. Without loss of generality, it is assumed that $\delta_m > 0$.

In the following of this paper, $h_0(u(k),x(k))$ is called the model uncertainties; $h_1(k,u(k),x(k))$ is called the unmodeled dynamics and denoted by $h_1(k)$; $h_2(k)$ is called the disturbance.

Remark 3.1 For the systems with uncertainties satisfying the above assumptions, adaptive pole placement control laws may be considered if ν is known [22,32]. The adaptive controller can work well even though the unknown parameters d_i and δ are not small. In this paper, a special adaptive pole placement control, i.e. the adaptive sliding mode control, is considered in order to make the best use of the merits of the adaptive control and the sliding mode control (the invariance property to the matched model uncertainties $h_0(u(k),x(k))$).

3.3 Discrete Quasi-Sliding Mode Adaptive Controller

In this section, first, the sliding surface is designed. Then, the parameters d_i and δ and the upper bound of $\|h_2(k)\|_2$ are estimated by using the adaptive algorithms with

dead-zones. Based on these estimates, the controller is determined to ensure the existence of the quasi-sliding mode along the surface $s(k)=0$ and the global stability of the closed-loop system in the sense that all the signals in the loop remain bounded.

3.3.1 Design of the Sliding Surface

The sliding surface is designed based on the philosophy proposed in [49]. For a symmetric positive definite matrix $P \in R^{n\times n}$, if we define

$$\|x(k)\|_P = \sqrt{x^T(k)Px(k)} \tag{3.15}$$

for the vector $x(k)$, the induced norm for a matrix $\Phi \in R^{n\times n}$ should be defined as

$$\|\Phi\|_P = \sqrt{\lambda_{\max}\left(P^{-1}\Phi^T P\Phi\right)}. \tag{3.16}$$

The vector G in (3.2) is defined by

$$G = b^T P, \tag{3.17}$$

where the symmetric positive definite matrix P should be chosen such that

$$\|A_{eq}\|_P = \|(I - b(b^T Pb)^{-1}b^T P)A\|_P < 1. \tag{3.18}$$

Let μ_0 and μ_1 denote the square roots of the minimum and maximum eigenvalues of the symmetric positive definite matrix P, respectively. Thus, from (3.13) and (3.14), it yields

$$\|h_1(k)\|_P \le \mu_1\|h_1(k)\|_2 \le \alpha\mu_1\{\|x(k)\|_2 + |u(k)|\} \le \alpha\mu_1\{\mu_0^{-1}\|x(k)\|_P + |u(k)|\} \tag{3.19}$$

$$\|h_2(k)\|_P \le \mu_1\|h_2(k)\|_2 \le \mu_1\nu \tag{3.20}$$

3.3.2 The Adaptive Algorithms

From Assumption 3.3, pre-multiplying (3.9) by $b^T P$ yields

$$s(k+1) = b^T PAx(k) + b^T Pbdx(k) + b^T Pb(1+\delta)u(k) + b^T P\{h_1(k)+h_2(k)\}. \tag{3.21}$$

By transferring the available terms to the left side and dividing the both sides by $b^T Pb$, the above equation gives

$$\begin{aligned}&(b^T Pb)^{-1}\{s(k+1) - b^T PAx(k)\}\\ &= d\cdot x(k) + (1+\delta)u(k) + (b^T Pb)^{-1}b^T P\{h_1(k)+h_2(k)\}.\end{aligned} \tag{3.22}$$

If we define

$$y(k+1) = (b^T Pb)^{-1}\{s(k+1) - b^T PAx(k)\}, \tag{3.23}$$

$$\phi(k) = [x^T(k), u(k)]^T, \tag{3.24}$$

$$\theta = [d,\gamma]^T,\ \ \gamma = 1+\delta, \tag{3.25}$$

then, Equation (3.22) can be rewritten as

$$y(k+1) = \phi(k)^T\theta + (b^T Pb)^{-1}b^T P\{h_1(k)+h_2(k)\}. \tag{3.26}$$

Let $\hat{\theta}(k) \triangleq [\hat{d}(k),\hat{\gamma}(k)]^T$ denote the estimate of the unknown parameter θ at instant k. Define the estimation error as

$$e(k) = y(k) - \phi^T(k-1)\hat{\theta}(k-1). \tag{3.27}$$

Thus, $e(k)$ can also be expressed as

$$e(k) = \phi^T(k-1)\{\theta - \hat{\theta}(k-1)\} + (b^T Pb)^{-1}b^T P\{h_1(k-1)+h_2(k-1)\}. \tag{3.28}$$

Suppose the upper bound of $\left|(b^T Pb)^{-1}b^T Ph_2(k-1)\right|$ is ρ for all $k \ge 1$. Because ρ is unknown, its estimate $\hat{\rho}(k-1)$ is used to construct the dead-zone function. Define

$$\hat{\eta}(k-1) = \alpha(b^T Pb)^{-1}\|Pb\|_2\{\|x(k-1)\|_2 + |u(k-1)|\} + \hat{\rho}(k-1). \tag{3.29}$$

The dead-zone function is defined as

$$\lambda(k) = \begin{cases} 1 - \dfrac{\hat{\eta}(k-1)}{|e(k)|} & |e(k)| > \hat{\eta}(k-1) \\ 0 & otherwise \end{cases} \tag{3.30}$$

Thus, $\hat{\rho}(k)$ can be intuitively updated by the following adaptation law

$$\hat{\rho}(k)=\hat{\rho}(k-1)+\varepsilon\cdot\lambda(k)\cdot|e(k)|, \tag{3.31}$$

where $0<\varepsilon<1$, $\hat{\rho}(0)$ can be any small positive constant.

The estimate $\hat{\theta}(k)$ of θ can be updated by the next adaptation law with projection [22]

$$\hat{\theta}^{'}(k)=\hat{\theta}(k-1)+\frac{\varepsilon\lambda(k)\phi(k-1)e(k)}{1+\phi^{T}(k-1)\cdot\phi(k-1)}, \tag{3.32}$$

$$\hat{\theta}(k)=proj\{\hat{\theta}^{'}(k)\}, \tag{3.33}$$

where $\hat{\theta}^{'}(k)=\left[\hat{d}^{'}(k),\hat{\gamma}^{'}\right]^{T}$, *proj* is the projection operator such that

$$proj\{\hat{d}^{'}(k)\}=\hat{d}^{'}(k), \tag{3.34}$$

$$proj\{\hat{\gamma}^{'}(k)\}=\begin{cases}\hat{\gamma}^{'}(k) & \hat{\gamma}^{'}(k)\geq\delta_{m}\\ \delta_{m} & otherwise\end{cases} \tag{3.35}$$

The entries of the initial condition $\hat{d}(0)$ can be any constants, while the initial condition of $\hat{\gamma}(k)$ should be chosen as $\hat{\gamma}(0)\geq\delta_{m}$.

By recalling the adaptation algorithm defined in (3.31), it can be seen that the update estimate $\hat{\rho}(k)$ of ρ is too sensitive to the difference $|e(k)|-\hat{\eta}(k-1)$. In practice, corresponding to the adaptation law of θ defined in (3.32)-(3.35), the update estimate of ρ in (3.31) is normalized as

$$\hat{\rho}(k)=\hat{\rho}(k-1)+\frac{\varepsilon\cdot\lambda(k)\cdot|e(k)|}{1+\phi^{T}(k-1)\cdot\phi(k-1)}. \tag{3.36}$$

Define

$$\tilde{\theta}(k)=\left[\tilde{d}(k),\tilde{\gamma}(k)\right]^{T}\triangleq\hat{\theta}(k)-\theta,\ \tilde{\rho}(k)\triangleq\hat{\rho}(k)-\rho,\ \tilde{\gamma}^{'}(k)=\hat{\gamma}^{'}(k)-\gamma. \tag{3.37}$$

Then, it can be easily seen that $\tilde{\gamma}^{2}(k)\leq\tilde{\gamma}^{'2}(k)$. Thus,

$$\tilde{\theta}^{T}(k)\tilde{\theta}(k)\leq\tilde{\theta}^{'T}(k)\tilde{\theta}^{'}(k). \tag{3.38}$$

Now, consider the Lyapunov function candidate

$$V(k)=\tilde{\theta}^{T}(k)\tilde{\theta}(k)+\tilde{\rho}^{2}(k). \tag{3.39}$$

Taking the difference of *V(k)* yields

$$\begin{aligned}
&V(k)-V(k-1)\\
&\leq\tilde{\theta}^{'T}(k)\tilde{\theta}^{'}(k)-\tilde{\theta}^{T}(k-1)\tilde{\theta}(k-1)+\{\tilde{\rho}(k)+\tilde{\rho}(k-1)\}\{\hat{\rho}(k)-\hat{\rho}(k-1)\}\\
&=\frac{\varepsilon\lambda(k)e(k)\phi^{T}(k-1)}{1+\phi^{T}(k-1)\cdot\phi(k-1)}\{2\tilde{\theta}(k-1)+\frac{\varepsilon\lambda(k)\phi(k-1)e(k)}{1+\phi^{T}(k-1)\cdot\phi(k-1)}\}\\
&+\frac{\varepsilon\lambda(k)|e(k)|}{1+\phi^{T}(k-1)\cdot\phi(k-1)}\{2\tilde{\rho}(k-1)+\frac{\varepsilon\lambda(k)|e(k)|}{1+\phi^{T}(k-1)\cdot\phi(k-1)}\}\\
&=\frac{2\varepsilon\lambda(k)\{e(k)\phi^{T}(k-1)\tilde{\theta}(k-1)+|e(t)|\tilde{\rho}(k-1)\}}{1+\phi^{T}(k-1)\cdot\phi(k-1)}+\frac{\varepsilon^{2}\lambda^{2}(k)e^{2}(k)}{1+\phi^{T}(k-1)\cdot\phi(k-1)}.
\end{aligned} \tag{3.40}$$

As

$$e(k)(b^{T}Pb)^{-1}b^{T}Ph_{2}(k-1)-|e(k)|\rho\leq 0, \tag{3.41}$$

then, by using the definitions of $\hat{\eta}(k-1)$ and $\lambda(k)$, it yields

$$\begin{aligned}
&\lambda(k)\{e(k)\phi^{T}(k-1)\tilde{\theta}(k-1)+|e(k)|\tilde{\rho}(k-1)\}\\
&=\lambda(k)\{e(k)\{(b^{T}Pb)^{-1}b^{T}P\{h_{1}(k-1)+h_{2}(k-1)\}-e(k)\}+|e(k)|\{\hat{\rho}(k-1)-\rho\}\}\\
&\leq\lambda(k)\{e(k)\|(b^{T}Pb)^{-1}|\cdot\|Pb\|_{2}\alpha\{|x(k-1)\|_{2}+|u(k-1)|\}-e^{2}(k)+|e(k)|\hat{\rho}(k-1)\}\\
&=-\lambda^{2}(k)e^{2}(k).
\end{aligned} \tag{3.42}$$

Therefore, substituting (3.42) into (3.40) yields

$$V(k)-V(k-1)\leq-\frac{\varepsilon\lambda^{2}(k)e^{2}(k)(2-\varepsilon)}{1+\phi^{T}(k-1)\cdot\phi(k-1)}. \tag{3.43}$$

Summing the both sides of relation (3.43) from $k=1$ to N gives

$$V(N)-V(0)\leq-(2-\varepsilon)\varepsilon\sum_{k=1}^{N}\frac{\lambda^{2}(k)e^{2}(k)}{1+\phi^{T}(k-1)\phi(k-1)}. \tag{3.44}$$

So, by the fact $V(N)>0$, the following properties can be obtained [22].

(P1). $\hat{\theta}(k)$ and $\hat{\rho}(k)$ are bounded for all $k \geq 0$.

(P2). $\hat{\gamma}(k) \geq \delta_m$.

(P3). $\lim_{N\to\infty} \sum_{k=1}^{N} \frac{\lambda^2(k)e^2(k)}{1+\phi^T(k-1)\phi(k-1)} < \infty$.

(P4). $\lim_{k\to\infty} \frac{\lambda^2(k)e^2(k)}{1+\phi^T(k-1)\phi(k-1)} = 0$.

Remark 3.2 If $\delta_m < 0$, the projection operator can be defined similarly. The above results, except (P2) which should be $\hat{\gamma}(k) \leq \delta_m$, can be derived.

3.3.3 The Quasi-Sliding Mode Control

From now on, the control input is determined so that the quasi-sliding mode exists along the sliding surface $s(k) = 0$.

In this paper, the adaptive control law is considered as

$$u(k) = \frac{-\left\{(b^T Pb)^{-1} b^T PA + \hat{d}(k)\right\}x(k)}{\hat{\gamma}(k)}. \tag{3.45}$$

Using the control (3.45), (3.9) can be described as

$$\begin{aligned} x(k+1) &= Ax(k) + bdx(k) + \frac{\gamma}{\hat{\gamma}(k)} b\left\{-\left\{(b^T Pb)^{-1} b^T PA + \hat{d}(k)\right\}x(k)\right\} + h_1(k) + h_2(k) \\ &= \left\{I - b(b^T Pb)^{-1} b^T P\right\}Ax(k) + \frac{\gamma - \hat{\gamma}(k)}{\hat{\gamma}(k)} b\left\{-\left\{(b^T Pb)^{-1} b^T PA + \hat{d}(k)\right\}x(k)\right\} \\ &\quad + b\left\{d - \hat{d}(k)\right\}x(k) + h_1(k) + h_2(k) \\ &= \left\{I - b(b^T Pb)^{-1} b^T P\right\}Ax(k) + b\left\{\gamma - \hat{\gamma}(k)\right\}u(k) \\ &\quad + b\left\{d - \hat{d}(k)\right\}x(k) + h_1(k) + h_2(k) \\ &= A_{eq}x(k) + b \cdot e(k+1) + \left\{I - b(b^T Pb)^{-1} b^T P\right\}\left\{h_1(k) + h_2(k)\right\}. \end{aligned} \tag{3.46}$$

Multiplying (3.46) by $b^T P$ yields

$$s(k+1) = b^T Pb \cdot e(k+1). \tag{3.47}$$

To analysis the stability of the system (3.9) controlled by (3.45), we cite the following Lemma (The Key Technical Lemma, [5]).

Lemma 3.1 If the following conditions are satisfied,

(1) $\lim_{k\to\infty} \frac{\beta^2(k)}{1+\varphi^T(k)\varphi(k)} = 0$,

(2) $\|\varphi(k)\|_2 = \left\{\varphi^T(k)\varphi(k)\right\}^{\frac{1}{2}} \leq \kappa_1 + \kappa_2 \max_{0\leq\tau\leq k} |\beta(\tau)|$,

where κ_1 and κ_2 are constants, it follows that $\lim_{k\to\infty} \beta(k) = 0$.

We have the following theorem to describe the stability of the controlled system.

Theorem 1. Consider the system (3.9) satisfying Assumptions (3.1)-(3.5) controlled by the adaptive controller described in (3.45). Then, there exists an upper bound $\overline{\alpha} > 0$ such that

(i) $\lim_{k\to\infty} \lambda(k)|e(k)| = 0$, i.e. $\limsup_{k\to\infty} \{|e(k)| - \hat{\eta}(k-1)\} \leq 0$,

(ii) all the signals in the loop remain bounded,

for the class of uncertainties (3.10) for any $\alpha > 0$ smaller than $\overline{\alpha}$.

Proof: By applying the properties (P1) and (P2), from (3.45), we can concluded that there exists a positive constant C_1 such that

$$|u(k)| \leq C_1 \|x(k)\|_P. \tag{3.48}$$

The proof is given for two possible cases.

Case 1: There exists an integer $K > 0$ such that $|e(k)| \leq \hat{\eta}(k-1)$, i.e. $\lambda(k) = 0$ for all $k > K$.

In this case, result (i) is obvious. From (3.46), it yields

$$\begin{aligned} \|x(k+1)\|_P &\leq \|A_{eq}\|_P \|x(k)\|_P + \|b\|_P \hat{\eta}(k) + \|I - b(b^T Pb)^{-1} b^T P\|_P \left(\|h_1(k)\|_P + \|h_2(k)\|_P\right) \\ &\leq \|A_{eq}\|_P \|x(k)\|_P + \|b\|_P \left\{\alpha (b^T Pb)^{-1} \|Pb\|_2 \left\{\|x(k)\|_2 + |u(k)|\right\} + \hat{\rho}(k)\right\} \\ &\quad + \|I - b(b^T Pb)^{-1} b^T P\|_P \mu_1 \left\{\alpha\left\{\mu_0^{-1} + C_1\right\}\|x(k)\|_P + \nu\right\} \\ &\leq \left\{\|A_{eq}\|_P + \alpha\Sigma\right\}\|x(k)\|_P + \|b\|_P \hat{\rho}(k) + \nu\mu_1 \|I - b(b^T Pb)^{-1} b^T P\|_P \end{aligned} \tag{3.49}$$

for all $k > K$, where (3.19), (3.20) and (3.48) are used, Σ is defined by

$$\Sigma = \left\{\mu_1 \left\| I - b(b^T Pb)^{-1} b^T P \right\|_P + (b^T Pb)^{-1} \|b\|_P \|Pb\|_2 \right\} \left(\mu_0^{-1} + C_1\right). \tag{3.50}$$

As $\hat{\rho}(k)$ is uniformly bounded, it can be seen that $x(k)$ is uniformly bounded (Thus, $u(k)$ is also uniformly bounded) if $\|A_{eq}\|_P + \alpha\Sigma < 1$. So, there exists a small positive constant $\bar{\alpha}$, which is not smaller than $\left\{1 - \|A_{eq}\|_P\right\} / \Sigma$, such that result (ii) holds if $\alpha < \bar{\alpha}$.

Case 2: There exists a subsequence k_i $(i = 1,2,\cdots)$ such that

$$|e(k_i + 1)| > \hat{\eta}(k_i) \text{ and } |e(k+1)| \le \hat{\eta}(k) \text{ for } k_i < k < k_{i+1}. \tag{3.51}$$

From Equation (3.46), we have

$$\begin{aligned}
\|x(k+1)\|_P &\le \|A_{eq}\|_P \|x(k)\|_P + \|b\|_P |e(k+1)| + \left\| I - b(b^T Pb)^{-1} b^T P \right\|_P \left(\|h_1(k)\|_p + \|h_2(k)\|_P \right) \\
&\le \|A_{eq}\|_P \|x(k)\|_P + \|b\|_P \left\{ |e(k+1)| - \hat{\eta}(k) \right\} + \|b\|_P \hat{\eta}(k) \\
&\quad + \mu_1 \left\| I - b(b^T Pb)^{-1} b^T P \right\|_P \left\{ \alpha(\mu_0^{-1} + C_1) \|x(k)\|_P + \nu \right\} \\
&\le \left\{ \|A_{eq}\|_P + \alpha\Sigma \right\} \|x(k)\|_P + \|b\|_P \left\{ |e(k+1)| - \hat{\eta}(k) \right\} + \|b\|_P \hat{\rho}(k) \\
&\quad + \nu\mu_1 \left\| I - b(b^T Pb)^{-1} b^T P \right\|_P
\end{aligned} \tag{3.52}$$

where (3.19), (3.20) and (3.48) are used. If $\|A_{eq}\|_P + \alpha\Sigma < 1$, by using the fact that $\hat{\rho}(k)$ is uniformly bounded, it can be concluded that there exist positive constants C_2 and C_3 such that

$$\|x(k)\|_P \le C_2 + C_3 \max_{0 \le \tau \le k} \left\{ |e(\tau)| - \hat{\eta}(\tau - 1) \right\} \le C_2 + C_3 \max_{0 \le \tau \le k} \left\{ |e(\tau + 1)| - \hat{\eta}(\tau) \right\}. \tag{3.53}$$

Thus, there exist positive constants C_4 and C_5 such that

$$\begin{aligned}
\|\phi(k)\|_2 &\le \|x(k)\|_2 + |u(k)| \\
&\le \mu_0^{-1} \|x(k)\|_P + |u(k)| \\
&\le C_4 + C_5 \max_{0 \le \tau \le k} \left\{ |e(\tau + 1)| - \hat{\eta}(\tau) \right\},
\end{aligned} \tag{3.54}$$

if $\|A_{eq}\|_P + \alpha\Sigma < 1$. Based on the above inequality and property (P4), by applying Lemma 1, it can be concluded that there exists a small positive constant $\bar{\alpha}$, which is not smaller than $\left\{1 - \|A_{eq}\|_P\right\} / \Sigma$, such that result (i) holds if $\alpha < \bar{\alpha}$.

By employing the result (i) and noticing the assumption of Case 2, it can be concluded that $\max_{0 \le \tau \le k} \left\{ |e(k+1)| - \hat{\eta}(k) \right\}$ is positive and uniformly bounded. Thus, from (3.54), it can be concluded that all the signals in the loop are uniformly bounded. Therefore, the theorem is proved.

Remark 3: By observing (3.47) and applying Theorem 1, it can be seen that the state oscillates in a region near the sliding surface due to the existence of uncertainties.

Remark 4: By observing the parameter adaptation law (3.32)-(3.35), the control input (3.45) and the Equation (3.47), it can be seen that in the region $|s(k)| \le (b^T Pb)^{-1} \hat{\eta}(k-1)$ near the sliding surface, the linear feedback coefficients at instant k are same as those at the former instant $k-1$. Outside of this region, the feedback coefficients are changed. Therefore, the proposed adaptive sliding mode control is indeed a switching one, where the dead-zone method plays an important role. The mechanism of the new controller is somewhat similar to that of the controller in [18]. But the new controller can cope with a much more general class of uncertainties than the controller in [18].

Corollary 3.1 Consider the system described in Theorem 1 if we know that the class of disturbance $h_2(k)$ is absent. Then, there exists an upper bound $\bar{\alpha} > 0$ such that the state of the system can be controlled to approach to zero asymptotically by using the controller (3.45) for the uncertainties $h_0(k)$ and $h_1(k)$ satisfying $\alpha < \bar{\alpha}$.

Proof: If we know that the class of disturbance $h_2(k)$ is absent, then $\nu = 0$ and $\hat{\rho}(k)$ can be set to zero for all k. The proof will be given for the two corresponding

cases presented in Theorem 3.1.

Case 1: In this case, (3.49) can be simplified as

$$\|x(k+1)\|_P \le \{\|A_{eq}\|_P + \alpha\Sigma\}\|x(k)\|_P. \tag{3.55}$$

It is obvious that the state $x(k)$ asymptotically approaches to zero if $\|A_{eq}\|_P + \alpha\Sigma < 1$.

Case 2: In this case, (3.52) is simplified as

$$\|x(k+1)\|_P \le \{\|A_{eq}\|_P + \alpha\Sigma\}\|x(k)\|_P + \|b\|_P\{|e(k+1)| - \hat{\eta}(k)\}. \tag{3.56}$$

Thus,

$$\|x(k+1)\|_P \le \begin{cases} \{\|A_{eq}\|_P + \alpha\Sigma\}\|x(k)\|_P & for\ k_i < k < k_{i+1} \\ \{\|A_{eq}\|_P + \alpha\Sigma\}\|x(k)\|_P + \|b\|_P\{|e(k+1)| - \hat{\eta}(k)\} & for\ k = k_i \end{cases} \tag{3.57}$$

Because, in this case, result (i) of Theorem 1 also implies that

$$0 < |e(k_i+1)| - \hat{\eta}(k_i) \to 0 \ (\text{as } i \to \infty), \tag{3.58}$$

it can be concluded that $x(k) \to 0$ (as $k \to \infty$) from (3.57) if $\|A_{eq}\|_P + \alpha\Sigma < 1$.

Thus, there exists an upper bound $\bar{\alpha}$, which is not smaller than $\{1 - \|A_{eq}\|_P\}/\Sigma$, such that $x(k) \to 0$ for the uncertainties $h_0(k)$ and $h_1(k)$ satisfying $\alpha < \bar{\alpha}$.

Corollary 3.2 Consider the system described in Theorem 3.1 if we know that $h_1(k)$ is of the form

$$h_1(k) = \bar{b}\,h_3(k), \quad |h_3(k)| \le \beta\{\|x(k)\|_2 + |u(k)|\}, \tag{3.59}$$

where $\bar{b} \in R^n$ is a known vector, $\beta > 0$ is a known constant. Then, by redefining the function $\hat{\eta}(k-1)$ in (3.29) as

$$\hat{\eta}'(k-1) = \beta(b^T Pb)^{-1}|b^T P\bar{b}|\{\|x(k-1)\|_2 + |u(k-1)|\} + \hat{\rho}(k-1), \tag{3.60}$$

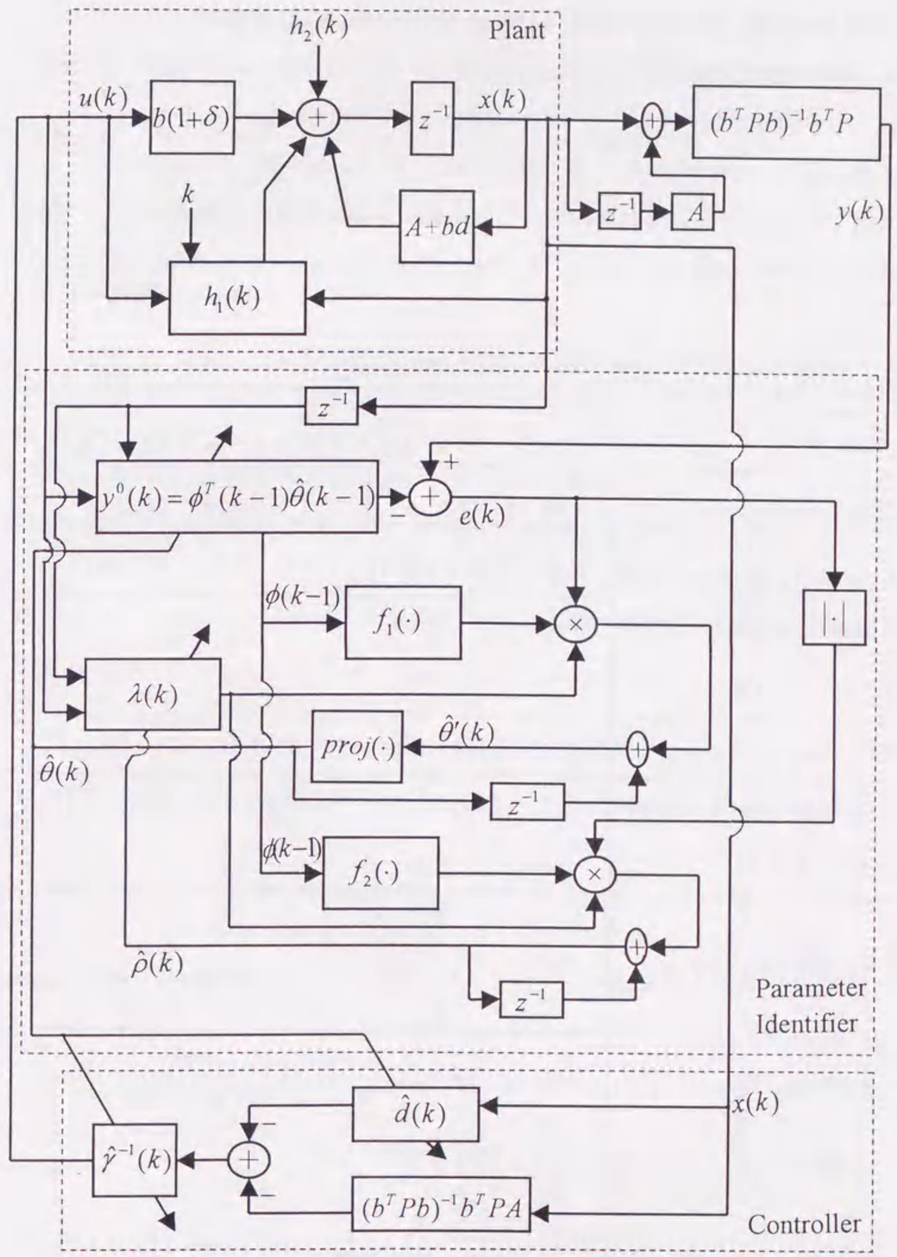

Fig. 3.1 The block diagram of the discrete-time adaptive quasi-sliding mode control system.

we can concluded that there exists an upper bound $\overline{\beta} > 0$ such that

(i) all the signals in the loop remain bounded,

(ii) the performance of the controller defined in (3.45) may become better,

for the class of uncertainties (3.10) satisfying (3.59) for any $\beta > 0$ smaller than $\overline{\beta}$.

Proof: Result (i) can be proved by a procedure similar to that of Theorem 3.1. It is easy to see that $\hat{\eta}'(k-1) \le \hat{\eta}(k-1)$. Thus, from Remark 3.3, result (ii) is obvious.

Table 3.1 The discrete-time adaptive quasi-sliding mode control algorithm

Plant	$x(k+1) = (A+bd)x(k) + b(1+\delta)u(k) + h_1(k) + h_2(k)$
Plant variable vector	$\phi(k) = \left[x^T(k),\ u(k)\right]^T$
Estimated parameter vector	$\hat{\theta}(k) = \left[\hat{d}(k),\ \hat{\gamma}(k)\right]^T$
Estimated upper bound of $\left\|(b^T Pb)^{-1} b^T P h_2(k-1)\right\|$	$\hat{\rho}(k)$
Estimation error signal	$e(k) = y(k) - \phi^T(k-1)\hat{\theta}(k-1)$
Estimated upper bound of $h_1(k) + h_2(k)$	$\hat{\eta}(k-1) = \alpha(b^T Pb)^{-1}\left\|Pb\right\|_2 \left\{\left\|x(k-1)\right\|_2 + \left\|u(k-1)\right\|\right\} + \hat{\rho}(k-1)$
Dead-zone function	$\lambda(k) = \begin{cases} 1 - \dfrac{\hat{\eta}(k-1)}{\left\|e(k)\right\|} & \left\|e(k)\right\| > \hat{\eta}(k-1) \\ 0 & otherwise \end{cases}$
Adaptation law	$\hat{\theta}'(k) = \hat{\theta}(k-1) + \dfrac{\varepsilon\lambda(k)\phi(k-1)e(k)}{1+\phi^T(k-1)\cdot\phi(k-1)}$ $\hat{\theta}(k) = proj\left\{\hat{\theta}'(k)\right\}$ $\hat{\rho}(k) = \hat{\rho}(k-1) + \dfrac{\varepsilon\cdot\lambda(k)\cdot\left\|e(k)\right\|}{1+\phi^T(k-1)\cdot\phi(k-1)}$
Control input	$u(k) = \dfrac{-\left\{(b^T Pb)^{-1} b^T PA + \hat{d}(k)\right\}x(k)}{\hat{\gamma}(k)}$

The block diagram of the discrete-time adaptive quasi-sliding mode control system is given in Figure 3.1, where, for a vector α, the functions $f_1(\alpha)$ and $f_2(\alpha)$ are defined as $f_1(\alpha) \triangleq \dfrac{\varepsilon\alpha}{1+\alpha^T\alpha}$ and $f_2(\alpha) \triangleq \dfrac{\varepsilon}{1+\alpha^T\alpha}$, respectively.

The algorithm proposed in this chapter can be summarized in table 3.1.

3.4 Simulation Results

This section presents an example and its simulation results to illustrate the proposed algorithm.

Consider the unstable discrete-time system described by

$$\begin{bmatrix} x_1(k+1) \\ x_2(k+1) \end{bmatrix} = \left\{\begin{bmatrix} 0 & 1 \\ 1.2 & 0.8 \end{bmatrix} + \begin{bmatrix} 0 \\ 1 \end{bmatrix} d\right\}\begin{bmatrix} x_1(k) \\ x_2(k) \end{bmatrix} + (1+\delta)\begin{bmatrix} 0 \\ 1 \end{bmatrix}u(k) + h_1(k) + h_2(k),$$

where $d = -[0.24, 0.4]$ and $\delta = 0.4$ are the unknown parameters; the uncertainties $h_1(k)$ and $h_2(k)$ are described by

$$h_1(k) = 0.1\sin(k)\left\{2u(k) + x_1(k) + x_2(k)\right\}\begin{bmatrix} 1 \\ 1 \end{bmatrix}$$

and

$$h_2(k) = 0.2\sin(k)\left\{0.4 + \frac{\left\|x(k)\right\|_2}{1+\left\|x(k)\right\|_2}\right\}\begin{bmatrix} 1 \\ 2 \end{bmatrix},$$

respectively. Suppose we know that $\left\|h_1(k)\right\|_2 \le 0.3\left\{\left\|x(k)\right\|_2 + \left\|u(k)\right\|\right\}$ and $\delta_m = 1$.

In the simulation process, the state starting at $x(0) = [1,1]^T$ is investigated. P is designed as $P = \begin{bmatrix} 1 & 1 \\ 1 & 4 \end{bmatrix}$. Thus, $\left\|A_{eq}\right\|_P = \left\|\begin{bmatrix} 0 & 1 \\ 0 & -0.25 \end{bmatrix}\right\|_P = 0.5$. ε is chosen as $\varepsilon = 0.9$. $\hat{\rho}(0)$ and $\hat{\theta}(0)$ are set to $\hat{\rho}(0) = 0.1$ and $\hat{\theta}(0) = [1,1,1]^T$. Figures 3.2 and 3.3 show the responses for the controlled states $x_1(k)$ and $x_2(k)$, respectively. Figure 3.4 shows the response for the variable $s(k)$. Figure 3.5 shows the quasi-

sliding mode control. It can be seen that there exist quasi-steady state oscillations due to the existence of disturbances.

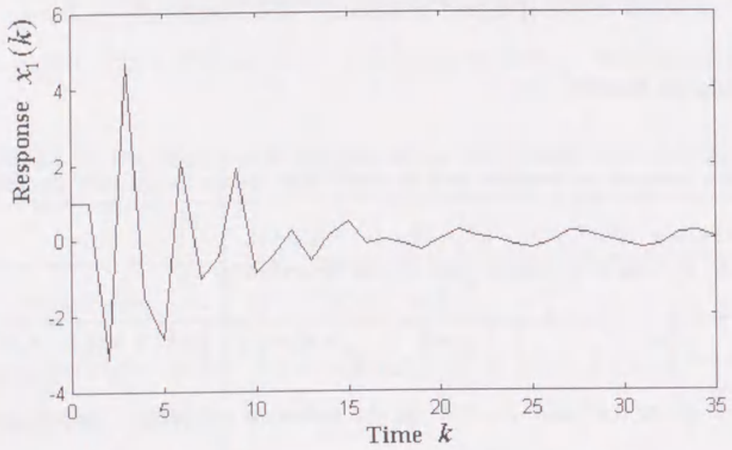

Fig. 3.2 The response for the controlled state $x_1(k)$.

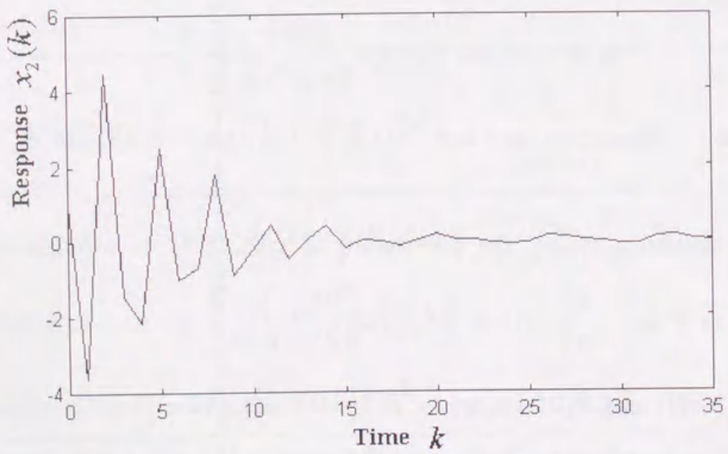

Fig. 3.3 The response for the controlled state $x_2(k)$.

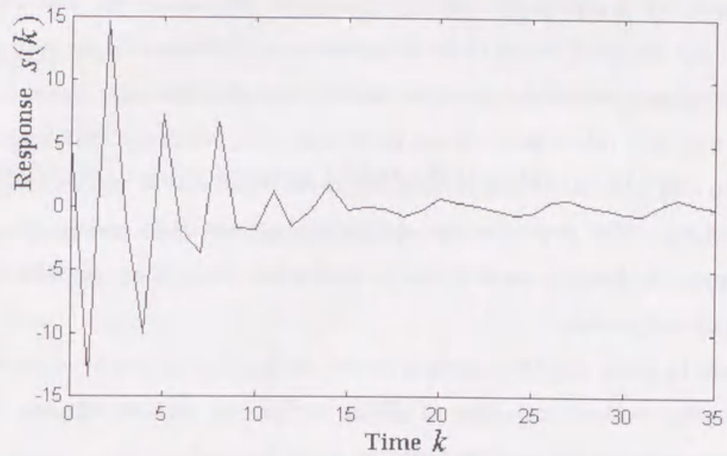

Fig.3.4 The response for the variable $s(k)$.

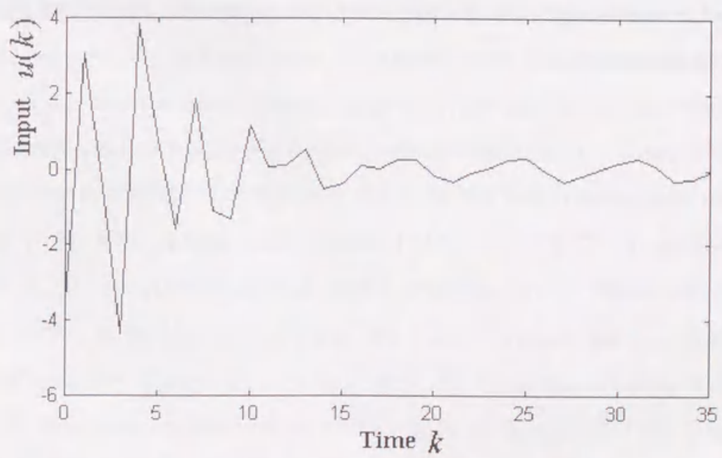

Fig. 3.5 The adaptive quasi-sliding mode control input.

3.5 Conclusions

In this paper, by applying the adaptive algorithms with dead-zone, the unknown parameters and the upper bound of the disturbances are estimated for the system with model uncertainties, unmodeled dynamics and bounded disturbances. Based on these estimates, a discrete robust quasi-sliding mode controller, which is a switching one, is proposed to guarantee the system to be stable in the sense that all signals in the loop remain bounded. The new controller makes the best use of the advantages of the adaptive control and sliding mode control. Simulation results show the effectiveness of the proposed algorithm.

It should be noted that the uncertain system in this chapter can be controlled by adaptive method without appealing to sliding modes, but such an adaptive control system does not posses the associate merits of the sliding mode.

If the unknown term $f(k, u(k), x(k))$ is matched and slow varying with respect to k, the proposed controller can be modified by using the techniques proposed in [2,14] to improve the control performance. The new controller can also be applied to servo control problems to achieve the output tracking. The proposed method is expected to be extended to input-output models with unknown parameters, unmodeled dynamics and bounded disturbances.

Chapter 4

Variable Structure System Theory Based Disturbance Identification and Its Applications

4.1 Introduction

In almost all engineering control systems, the presence of disturbances, model uncertainties and nonlinear model parts is inevitable. For example, when the robot manipulators grasp an unknown payload, they are affected by unknown inertia variation and gravity force. But these changes are rarely captured in the models. It is most desirable that the controllers be insensitive to these uncertainties. Thus, in recent years, the problem of controlling uncertain dynamical systems subject to external disturbances has been a topic of considerable interest. Many robust control methods are proposed. Among these methods, the most typical ones may be H_∞ control [3,8], VSS sliding mode control [12,13,20,24,26,57,71], adaptive control [22,27,31,32], μ-synthesis method [4,52], dynamic versus parametric uncertainty control [7,27], robust process control [6,51]. These methods can cope with different types of uncertain systems [7]. In this paper, the model uncertainties, the nonlinear parts of the system and the external disturbances are merged into one term, and we refer it as the disturbances of the system. It might be argued that if the disturbances can be estimated, the control problems of the systems with disturbances may become

easier to solve. For example, the state observer and the controller with disturbance cancellation functions can be easily constructed by using the estimated disturbances.

Among the many presented disturbance observer techniques, the approximate differentiator type [53,63] and H_∞ type [37] formulations have been popularly applied in the design of tracking controllers for motion control systems. The procedure of the first approach closes an inner loop around the controlled plant to reject disturbances and force the input-output character of this inner loop to approximate a "nominal" plant model at low frequencies. Tuning of the loop is accomplished through adjustment of a low pass filter. Since the plant approximates a nominal model at low frequencies, overall closed loop dynamics are usually well known and feedforward techniques are often applied. But there are some shortcomings of this approach. A fatal one is that a satisfactory control can hardly be obtained when the types of the disturbances are unknown and the model uncertainties exist [63]. Another is that the proposed formulation can only cope with some low frequency disturbances. The second approach makes the best use of the merits in H_∞ control [37]. The shortcoming of this approach is that it can only cope with step type disturbances.

From the point of view of robust control, the desirable properties of variable structure control systems are well documented in [26,55,57,71]. The advantage of this approach lies in that only the upper and lower bounds of the uncertainties are required. It should be pointed out that the equivalent control method is very effective for estimating the unknown parts of a plant with known relative degrees. So, we are inspired to apply the VSS theory to the disturbance observer formulation. It is known that the disturbance can be estimated by using the VSS equivalent control theory for minimum-phase dynamical systems with relative degree one (with respect to the relationship between the disturbance and output) [56,57]. But for the systems with higher relative degrees, no result has been reported. Usually, it is regarded impossible. This is because that the VSS type estimations are constructed by discontinuous functions.

For another important system identification problem "state observer formulation",

it is well known that the state observers can only be formulated only for the uncertain minimum phase systems with relative degree one [10,11,57,59,60,61]. In this chapter, by using the estimate of the disturbance, the state observer is formulated for the systems with arbitrarily relative degrees.

In this chapter, a disturbance estimation method based on the VSS equivalent control is proposed for the minimum-phase dynamical systems (with respect to the relationship between the disturbance and output) with arbitrary relative degrees. Only the upper and lower bounds of the disturbance are assumed to be known as the *a priori* information. By first estimating the higher order filters of the disturbance, the lower order filters of the disturbance are inductively estimated. Eventually, the disturbance is estimated. In the proposed formulation, the traditional discontinuous methods are approximated by differentiable approaches. The estimation error can be designed as small as it is needed.

The organization of this chapter is as follows. Section 4.2 gives the problem formulation. Section 4.3 presents the proposed robust disturbance observer for the minimum phase dynamical systems. In section 4.4, the discontinuous estimates are approximately modified. In section 4.5, the behavior of the new disturbance observer is tested by computer simulations. In section 4.6, the disturbance estimation algorithm is extended to nonminimum phase systems with arbitrarily relative degrees. In section 4.7, the estimated disturbance is applied to construct a state observer. In section 4.8, a pole assignment controller is established to place desired poles and to cancel the disturbance for the systems with matched disturbance. Section 4.9 gives a design example and its simulation results. In section 4.10, experiments are carried out to verify the practicality and effectiveness of the proposed approach. Also, the performances of the proposed observer and the traditional observer are compared.

4.2 Problem Statement

Consider an uncertain system of the form

$$\begin{cases} \dot{x}(t) = Ax(t) + bu(t) + kv(x,u,t), \quad x(t_0) = x_0 \\ y(t) = c^T x(t) \end{cases} \tag{4.1}$$

where $x(t)$ is an unknown state vector with known dimension n; $u(t)$ and $y(t)$ are scalar input and output, respectively; $v(x,u,t)$ represents the model uncertainties, the nonlinearities and the disturbance; t_0 is the starting time; x_0 is the unknown initial vector of the state $x(t)$; A, b, k, c are known matrices and are described in the observable canonical form

$$A = \begin{bmatrix} -a_1 & 1 & 0 & \cdots & 0 \\ -a_2 & 0 & 1 & \cdots & 0 \\ \cdot & \cdot & \cdot & \cdots & \cdot \\ -a_{n-1} & 0 & 0 & \cdots & 1 \\ -a_n & 0 & 0 & \cdots & 0 \end{bmatrix} \triangleq \begin{bmatrix} -a & I \\ \hline 0 & \end{bmatrix}, \quad b = \begin{bmatrix} b_1 \\ \vdots \\ b_n \end{bmatrix}, \quad k = \begin{bmatrix} k_1 \\ \vdots \\ k_n \end{bmatrix} \tag{4.2}$$

$$c = [1,0,\cdots,0]^T, \quad |v(x,u,t)| \le \rho(y,u,t) \tag{4.3}$$

where $\rho(y,u,t) \ge 0$ is a known function.

Define

$$a(s) = s^n + a_1 s^{n-1} + \cdots + a_n \tag{4.4}$$

$$b(s) = b_1 s^{n-1} + b_2 s^{n-2} + \cdots + b_n \tag{4.5}$$

$$k(s) = k_1 s^{n-1} + k_2 s^{n-2} + \cdots + k_n \tag{4.6}$$

Equation (4.1) also gives

$$a(s)y(t) = b(s)u(t) + k(s)v(x,u,t) \tag{4.7}$$

where s denotes the differential operator with respect to time t.

For simplicity, $v(x,u,t)$ is denoted by $v(t)$ and is referred to the disturbance of the system (4.1) in the following sections of this chapter.

This chapter attempts to estimate the disturbance by using the VSS equivalent control method even if $k_1 = 0$. Then, it is considered to apply the estimate of the disturbance to formulate a state observer and construct a pole assignment controller of system (4.1).

4.3 Disturbance Identification

In this section, only the minimum-phase systems (with respect to the relationship of disturbance-output, i.e. $k(s)$ is a Hurwitz polynomial) will be studied. The disturbance will be estimated by using the VSS theory.

4.3.1 An Introductory Example

In the following, an example is given to introduce the proposed recursive procedure by using the basic VSS control theory. Consider the system described by

$$(s^2 + a_1 s + a_2)y(t) = v(t) \tag{4.8}$$

where $v(t)$ is unknown, $|v(t)| \le \rho(t)$, but $\rho(t)$ is known. Our purpose is to estimate $v(t)$ by using the measurement of the output $y(t)$ and the *a priori* knowledge $\rho(t)$.

Inspired by the formulation of the state observer for a possibly unstable system [30], we introduce a Hurwitz polynomial $f(s) = (s+\lambda)^2$, $\lambda > 0$. Thus, (4.8) can be rewritten as

$$\dot{y}(t) + \lambda y(t) = \frac{(2\lambda - a_1)s + (\lambda^2 - a_2)}{s+\lambda} y(t) + \frac{1}{s+\lambda} v(t) \tag{4.9}$$

Step 1 Corresponding to (4.9), consider the following model

$$\dot{\hat{y}}(t) + \lambda \hat{y}(t) = \frac{(2\lambda - a_1)s + (\lambda^2 - a_2)}{s+\lambda} y(t) + w_1(t) \tag{4.10}$$

where $w_1(t)$ is the input chosen as $w_1(t) = \left\{ \frac{1}{s+\lambda} \rho(t) \right\} \operatorname{sgn}\{y(t) - \hat{y}(t)\}$ (the fact $\left| \frac{1}{s+\lambda} v(t) \right| \le \frac{1}{s+\lambda} \rho(t)$ is used). Then, it is easy to prove that $y(t) - \hat{y}(t) \to 0$ (as $t \to \infty$). By using the equivalent control method [56], $w_1(t)$ can be regarded as the estimate of $\frac{1}{s+\lambda} v(t)$. The above approach is the traditional standard VSS

type disturbance estimation method.

Step 2 By employing $w_1(t)$, we want to estimate the disturbance $v(t)$. Based on the following identical differential equation

$$\frac{d}{dt}\left\{\frac{1}{s+\lambda}v(t)\right\}+\frac{\lambda}{s+\lambda}v(t)=v(t) \tag{4.11}$$

we consider the dynamical system described by

$$\dot{\hat{w}}_1(t)+\lambda\hat{w}_1(t)=w_2(t),\quad \hat{w}_1(t_0)=0 \tag{4.12}$$

where $\hat{w}_1(t)$ is the estimate of $\frac{1}{s+\lambda}v(t)$, $w_2(t)$ is the input.

If $w_2(t)$ is chosen as $w_2(t)=\rho(t)\operatorname{sgn}\left\{\frac{1}{s+\lambda}v(t)-\hat{w}_1(t)\right\}$, then it can be easily proved that $\frac{1}{s+\lambda}v(t)-\hat{w}_1(t)\to 0$, where the problem is that $\frac{1}{s+\lambda}v(t)$ is

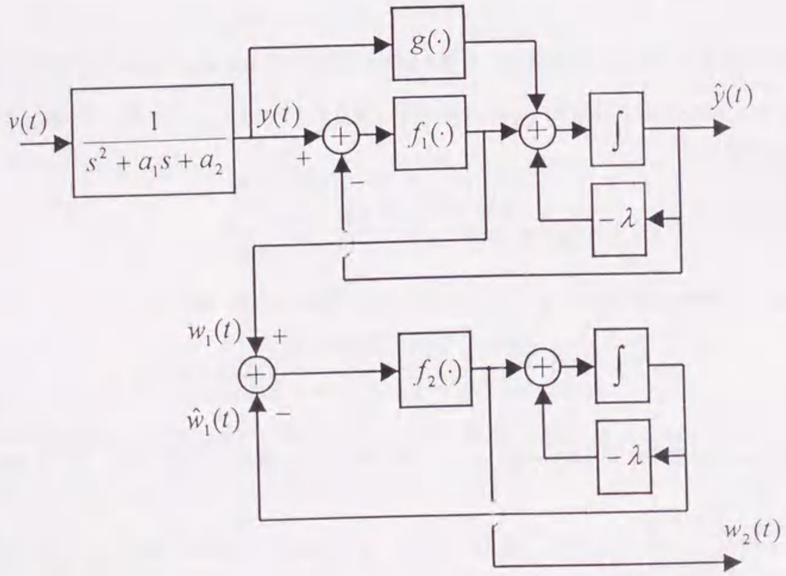

Fig. 4.1 The block diagram of the new observer for the two order input unknown system with relative degree two.

not an available signal. But, as $w_1(t)$ is the estimate of $\frac{1}{s+\lambda}v(t)$, we are inspired to replace $\frac{1}{s+\lambda}v(t)$ by $w_1(t)$ in the control input $w_2(t)$. Thus, the input $w_2(t)$ should be chosen as $w_2(t)=\rho(t)\operatorname{sgn}\{w_1(t)-\hat{w}_1(t)\}$. Figure 4.1 shows the design block diagram for this disturbance observer, where, for a variable $\mu(t)$, the functions $g(\cdot)$, $f_1(\cdot)$ and $f_2(\cdot)$ are defined as $g(\mu(t))\triangleq\frac{(2\lambda-a_1)s+(\lambda^2-a_2)}{s+\lambda}\mu(t)$, $f_1(\mu(t))=\left\{\frac{1}{s+\lambda}\rho(t)\right\}\operatorname{sgn}(\mu(t))$ and $f_2(\mu(t))=\rho(t)\cdot\operatorname{sgn}(\mu(t))$, respectively.

4.3.2 The Disturbance Identification Algorithm

Motivated by the introduced example, the general recursive design method employing integrators is proposed in this section. In the i-th step, the $(r\text{-}i)$-th order filter of the disturbance is estimated. In the final r-th step, the disturbance is estimated. As the VSS method is employed, the upper and lower bounds of the filters of the disturbance must be estimated.

For positive constant λ, $\frac{1}{s+\lambda}\rho(y(t),u(t),t)$ can be calculated as

$$\frac{1}{s+\lambda}\rho(y(t),u(t),t)=\int_{t_0}^{t}e^{-\lambda(t-\tau)}\rho(y(\tau),u(\tau),\tau)d\tau \tag{4.13}$$

By applying

$$\frac{1}{(s+\lambda)^i}\rho(y(t),u(t),t)=\frac{1}{s+\lambda}\left\{\frac{1}{(s+\lambda)^{i-1}}\rho(y(t),u(t),t)\right\} \tag{4.14}$$

the next lemma can be easily obtained.

Lemma 4.1 The upper bound of $\left|\frac{1}{(s+\lambda)^i}v(t)\right|$ can be estimated as

$$\left|\frac{1}{(s+\lambda)^r}v(t)\right| \le \frac{1}{(s+\lambda)^r}\rho(y(t),u(t),t) \triangleq \omega_r(t) \tag{4.15}$$

Remark 4.1 By the definition in (4.15), it is obvious that $\omega_0(t) = \rho(y(t),u(t),t)$. For the Hurwitz polynomial $k(s)$, suppose $k_r \neq 0$ and $k_i = 0$ for $i \le r-1$.

Inspired by the techniques introduced in [30], we introduce a Hurwitz polynomial as

$$f(s) = s^n + f_1 s^{n-1} + \cdots + f_n = \frac{1}{k_r}k(s)(s+\lambda)^r \tag{4.16}$$

Dividing the both sides of (4.7) by $f(s)$ yields

$$y(t) = \frac{f(s)-a(s)}{f(s)}y(t) + \frac{b(s)}{f(s)}u(t) + \frac{k_r}{(s+\lambda)^r}v(t) \tag{4.17}$$

Multiplying (4.17) by $s+\lambda$ yields

$$\dot{y}(t) + \lambda y(t) = k_r\left\{\frac{f(s)-a(s)}{k(s)(s+\lambda)^{r-1}}y(t) + \frac{b(s)}{k(s)(s+\lambda)^{r-1}}u(t)\right\} + \frac{k_r}{(s+\lambda)^{r-1}}v(t) \tag{4.18}$$

Let us consider the next differential equation

$$\dot{\hat{y}}(t) + \lambda\hat{y}(t) = k_r\left\{\frac{f(s)-a(s)}{k(s)(s+\lambda)^{r-1}}y(t) + \frac{b(s)}{k(s)(s+\lambda)^{r-1}}u(t)\right\} + k_r w_1(t) \tag{4.19}$$

where $\hat{y}(t)$ is the estimate of $y(t)$, $w_1(t)$ is the input to be determined. For simplicity, the initial condition of $\hat{y}(t)$ is set to zero. Combining (4.18) and (4.19) yields

$$\dot{\bar{y}}(t) + \lambda\bar{y}(t) = k_r\left\{\frac{1}{(s+\lambda)^{r-1}}v(t) - w_1(t)\right\} \tag{4.20}$$

where $\bar{y}(t) = y(t) - \hat{y}(t)$ is an available signal.

Now, $w_1(t)$ is chosen as

$$w_1(t) = \omega_{r-1}(t)\cdot \mathrm{sgn}(k_r\bar{y}(t)) \tag{4.21}$$

It can be proved that $\bar{y}(t)$ approaches zero asymptotically, i.e. a sliding mode exists on $\bar{y}(t) = 0$. In fact, from (4.20),

$$\begin{aligned}\frac{d}{dt}(\bar{y}(t))^2 &= -2\lambda(\bar{y}(t))^2 + 2\bar{y}(t)k_r\left\{\frac{1}{(s+\lambda)^{r-1}}v(t) - w_1(t)\right\}\\ &= -2\lambda(\bar{y}(t))^2 + 2\bar{y}(t)k_r\frac{1}{(s+\lambda)^{r-1}}v(t) - 2|\bar{y}(t)k_r|\omega_{r-1}(t)\\ &\le -2\lambda(\bar{y}(t))^2\end{aligned}$$

Thus, it is obvious that $\bar{y}(t)$ converges to zero exponentially.

In order to derive the sliding equations through the equivalent control method, it is necessary to solve

$$\frac{d}{dt}\bar{y}(t) = 0 \tag{4.22}$$

from (4.20) with respect to $w_1(t)$, and it yields

$$w_{1eq}(t) = \frac{1}{(s+\lambda)^{r-1}}v(t) \tag{4.23}$$

So, $w_1(t)$ can be regarded as the estimate of $\frac{1}{(s+\lambda)^{r-1}}v(t)$.

Now, we will use $w_1(t)$ to estimate $\frac{1}{(s+\lambda)^{r-2}}v(t)$ by appealing to the following identical differential equation.

$$\frac{d}{dt}\left\{\frac{1}{(s+\lambda)^{r-1}}v(t)\right\} + \frac{\lambda}{(s+\lambda)^{r-1}}v(t) = \frac{1}{(s+\lambda)^{r-2}}v(t) \tag{4.24}$$

Corresponding to (4.24), we consider the differential equation

$$\dot{\hat{w}}_1(t) + \lambda\hat{w}_1(t) = w_2(t) \tag{4.25}$$

where $\hat{w}_1(t)$ is the signal generated by (4.25), $w_2(t)$ is the input to be determined, and the initial condition of $\hat{w}_1(t)$ is set to zero. Denote $\bar{w}_1(t) = \frac{1}{(s+\lambda)^{r-1}}v(t) - \hat{w}_1(t)$, then from (4.24) and (4.25), we have

$$\dot{\overline{w}}_1(t) + \lambda \overline{w}_1(t) = \frac{1}{(s+\lambda)^{r-2}} v(t) - w_2(t) \tag{4.26}$$

The next lemma gives an input of $w_2(t)$ to force the error $\overline{w}_1(t)$ to converge to zero.

Lemma 4.2 If $w_2(t)$ is chosen as

$$w_2(t) = \omega_{r-2}(t) \cdot \mathrm{sgn}\{w_1(t) - \hat{w}_1(t)\} \tag{4.27}$$

then

$$\overline{w}_1(t) \to 0 \quad (\text{as } t \to \infty).$$

Proof: The proof is given in the Appendix.

Remark 4.2 As $\frac{1}{(s+\lambda)^{r-1}} v(t)$ is not available, its available estimate $w_1(t)$ is used to replace it in the determination of $w_2(t)$ in (4.27).

In order to derive the sliding equations through the equivalent control method, it is necessary to solve

$$\frac{d}{dt}\overline{w}_1(t) = 0 \tag{4.28}$$

in (4.26) with respect to $w_2(t)$, and it yields

$$w_{2eq}(t) = \frac{1}{(s+\lambda)^{r-2}} v(t) \tag{4.29}$$

So, $w_2(t)$ can be regarded as the estimate of $\frac{1}{(s+\lambda)^{r-2}} v(t)$.

By mathematical induction, we can construct the differential equation

$$\dot{\hat{w}}_{i-1}(t) + \lambda \hat{w}_{i-1}(t) = w_i(t) \tag{4.30}$$

where $\hat{w}_{i-1}(t)$ $(2 \le i \le r)$ is a measurable variable with the initial condition $\hat{w}_{i-1}(t_0) = 0$, $w_i(t)$ is determined as

$$w_i(t) = \rho(y(t), t) \cdot \mathrm{sgn}\{w_{i-1}(t) - \hat{w}_{i-1}(t)\} \tag{4.31}$$

By similar analysis, $w_i(t)$ can be regarded as the estimate of $\frac{1}{(s+\lambda)^{r-i}} v(t)$. The above analysis can be summarized in the next theorem.

Theorem 4.1 For the case that $k(s)$ is a Hurwitz polynomial, construct the following differential equations

$$\dot{\hat{y}}(t) + \lambda \hat{y}(t) = k_r \left\{ \frac{f(s) - a(s)}{k(s)(s+\lambda)^{r-1}} y(t) + \frac{b(s)}{k(s)(s+\lambda)^{r-1}} u(t) \right\} + k_r w_1(t) \tag{4.19}$$

$$\dot{\hat{w}}_{i-1}(t) + \lambda \hat{w}_{i-1}(t) = w_i(t) \quad (\text{for } 2 \le i \le r) \tag{4.32}$$

where $\hat{y}(t)$ and $\hat{w}_{i-1}(t)$ $(2 \le i \le r)$ are available variables with the initial conditions $\hat{y}(t_0) = 0$ and $\hat{w}_{i-1}(t_0) = 0 (2 \le i \le r)$, w_1 and $w_i(t)$ $(2 \le i \le r)$ are given by

$$w_1(t) = \omega_{r-1}(t) \cdot \mathrm{sgn}(k_r(y(t) - \hat{y}(t))) \tag{4.21}$$

and

$$w_i(t) = \omega_{r-i}(t) \cdot \mathrm{sgn}\{w_{i-1}(t) - \hat{w}_{i-1}(t)\} \text{ (for } 2 \le i \le r) \tag{4.33}$$

respectively. It can be concluded that $w_i(t)$ are the corresponding estimates of $\frac{1}{(s+\lambda)^{r-i}} v(t)$ for $1 \le i \le r$. Particularly, $w_r(t)$ is the estimate of the disturbance $v(t)$.

4.4 Modification of the Disturbance Identification Algorithm

In practice, as the discontinuous function $\mathrm{sgn}(\eta)$ can not be implemented by a digital computer, it must be approximately smoothened. Corresponding to Theorem 4.1, the next theorem is obtained.

Theorem 4.2 For the case that $k(s)$ is a Hurwitz polynomial, construct the following dynamical systems described by

$$\dot{\hat{y}}(t) + \lambda \hat{y}(t) = k_r \left\{ \frac{f(s) - a(s)}{k(s)(s+\lambda)^{r-1}} y(t) + \frac{b(s)}{k(s)(s+\lambda)^{r-1}} u(t) \right\}$$

$$+ k_r w_1(t), \quad \hat{y}(t_0) = 0 \tag{4.34}$$

$$\dot{\hat{w}}_{i-1}(t) + \lambda \hat{w}_{i-1}(t) = w_i(t), \ \hat{w}_{i-1}(t_0) = 0, \text{ for } 2 \le i \le r \tag{4.35}$$

where $w_1(t)$ and $w_i(t)$ $(2 \le i \le r)$ are given by

$$w_1(t) = \frac{k_r \{y(t) - \hat{y}(t)\} \omega_{r-1}^2(t)}{|k_r \{y(t) - \hat{y}(t)\}| \omega_{r-1}(t) + \delta_1}, \ \delta_1 > 0 \tag{4.36}$$

and

$$w_i(t) = \frac{\{w_{i-1}(t) - \hat{w}_{i-1}(t)\} \omega_{r-i}^2(t)}{|w_{i-1}(t) - \hat{w}_{i-1}(t)| \omega_{r-i}(t) + \delta_i}, \ \delta_i > 0, \text{ for } 2 \le i \le r \tag{4.37}$$

respectively; $\hat{y}(t)$ and $\hat{w}_{i-1}(t)$ $(2 \le i \le r)$ are signals generated by Equations (4.34) and (4.35), respectively. It can be concluded that, when $\sum_{i=1}^{r} \delta_i$ is very small, $w_i(t)$ can be approximately regarded as the corresponding estimates of $\frac{1}{(s+\lambda)^{r-i}} v(t)$ for $1 \le i \le r$ as t is large enough. Particularly, $w_r(t)$ is the approximate estimate of $v(t)$. Therefore, there exist $T_i > t_0$ and $\varepsilon_i(\delta_1, \cdots, \delta_i) > 0$ such that

$$\left| \frac{1}{(s+\lambda)^{r-i}} v(t) - w_i(t) \right| \le \varepsilon_i(\delta_1, \cdots, \delta_i) \tag{4.38}$$

where $\varepsilon_i(\delta_1, \cdots, \delta_i) \to 0$ as $\sum_{j=1}^{i} \delta_j \to 0$, for $1 \le i \le r$.

Proof: For the proof, see the Appendix.

The block diagram of the modified disturbance identifier for the minimum phase dynamical systems with relative degree r is shown in Figure 4.2, where, for a variable $\alpha(t)$, the functions $f_1(\cdot)$ and $f_i(\cdot)$ (for $i = 2, \cdots, r$) are defined as $f_1(\alpha(t)) \triangleq \frac{k_r \alpha(t) \cdot \omega_{r-1}^2(t)}{|k_r \alpha(t)| \omega_{r-1}(t) + \delta_1}$ and $f_i(\alpha(t)) \triangleq \frac{\alpha(t) \cdot \omega_{r-i}^2(t)}{|\alpha(t)| \omega_{r-i}(t) + \delta_1}$ (for $i = 2, \cdots, r$), respectively.

The modified disturbance identification algorithm is illustrated in Table 4.1.

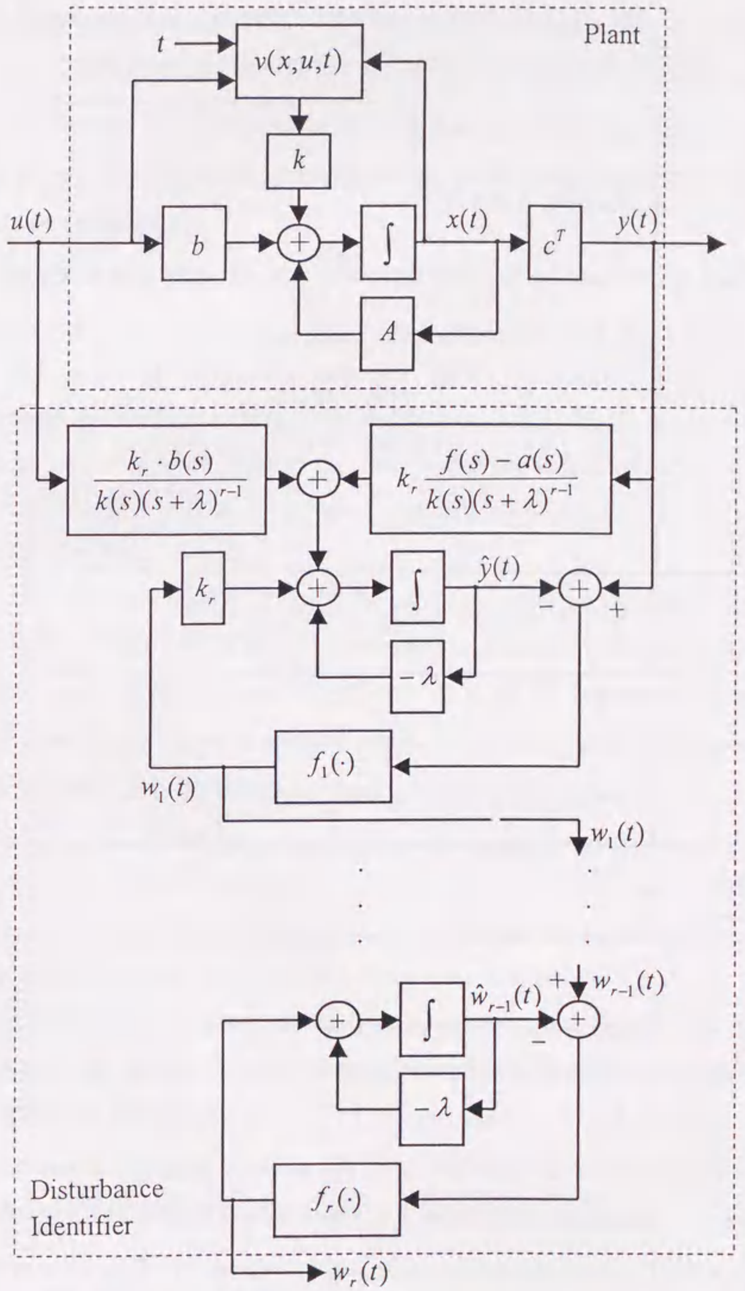

Fig. 4.2 The block diagram of the modified disturbance identifier for the minimum phase dynamical systems with relative degree r.

Table 4.1 The algorithm of the modified disturbance identification method for the minimum phase dynamical systems with relative degree r.

Plant	$a(s)y(t) = b(s)u(t) + k(s)v(x,u,t)$
A priori information	$\lvert v(x,u,t)\rvert \le \rho(y,u,t)$ (Thus, $\left\lvert \frac{1}{(s+\lambda)^r} v(t)\right\rvert \le \frac{1}{(s+\lambda)^r}\rho(y(t),u(t),t) \triangleq \omega_r(t)$)
Step 1:	$\dot{\hat{y}}(t) + \lambda\hat{y}(t) = k_r\left\{\frac{f(s)-a(s)}{k(s)(s+\lambda)^{r-1}} y(t) + \frac{b(s)}{k(s)(s+\lambda)^{r-1}} u(t)\right\} + k_r w_1(t), \quad w_1(t) = \frac{k_r\{y(t)-\hat{y}(t)\}\omega_{r-1}^2(t)}{\lvert k_r\{y(t)-\hat{y}(t)\}\rvert\omega_{r-1}(t)+\delta_1}$
Step 2:	$\dot{\hat{w}}_1(t) + \lambda\hat{w}_1(t) = w_2(t), \quad w_2(t) = \frac{\{w_1(t)-\hat{w}_1(t)\}\omega_{r-2}^2(t)}{\lvert w_1(t)-\hat{w}_1(t)\rvert\omega_{r-2}(t)+\delta_2}$
• • •	
Step r:	$\dot{\hat{w}}_{r-1}(t) + \lambda\hat{w}_{r-1}(t) = w_r(t), \quad w_r(t) = \frac{\{w_{r-1}(t)-\hat{w}_{r-1}(t)\}\omega_0^2(t)}{\lvert w_{r-1}(t)-\hat{w}_{r-1}(t)\rvert\omega_0(t)+\delta_r}$
Estimated disturbance	$w_r(t)$

Remark 4.3 Theorem 4.2 gives an approximate disturbance estimation method for minimum phase dynamical systems with arbitrarily relative degrees by using the VSS theory. The smaller the parameters δ_i $(1 \le i \le r)$ are chosen, the smaller the estimate error of the disturbance will be. For the high frequency disturbances, the parameters δ_i should be chosen to be very small in order to get good estimates.

Remark 4.4 The design parameter λ should be chosen to be large enough to raise the estimating speed (see (A62) and (A69)) if the controlled systems require. But if λ is chosen t o be too large, the estimation precision may become bad. This is because the estimation error is determined by $\dot{\bar{y}}(t) + \lambda\bar{y}(t)$ and $\dot{\bar{w}}_i(t) + \lambda\bar{w}_i(t)$. By referring to the proof of Theorem 4.2, it can be see that, although $\bar{y}(t)$ and $\bar{w}_i(t)$ can be made very small, $\lambda\bar{y}(t)$ and $\lambda\bar{w}_i(t)$ may not be very small when λ is chosen large. Simulation results will show how the performance of the new observer depends on the parameter λ.

Remark 4.5 Only the *a priori* information about the upper bound of $\lvert v(t)\rvert$ is required in our new formulation. We do not care which kind of disturbance it is. While the traditional disturbance observers should be designed differently (i.e. Different orders) for different types of disturbances in order to get good estimates [63]. As we can hardly know the types of the disturbances and the disturbances are usually composed of various types of signals, it is very difficult to determine the order of the traditional disturbance observer.

Remark 4.6 We need not to consider the variations of the model parameters in the new observer. The varying parts are regarded as a part of the disturbance. The polynomial $a(s)$ is not important to us, only its order n and the assumption that $k(s)$ is a Hurwitz polynomial are important to us. As a matter of fact, $a(s)$ is replaced by a designed Hurwitz polynomial $f(s)$ in our formulation.

Remark 4.7 From Remarks 4.5 and 4.6, we can conclude that the new disturbance observer is of high robustness with respect to the types of the disturbances and model uncertainties. By referring [63], it can be concluded that the new observer works like the imaginary traditional observer with infinity order theoretically.

Until now, the discussions are based on the theoretical analysis which is in the analog case. In the next section, computer simulations results will be present to illustrate the new formulation.

4.5 Test of the Disturbance Identification Algorithm

For simplicity, we consider the next system

$$s^2 y(t) = v(t) \tag{4.39}$$

where $|v(t)| \le \rho(t)$ and the starting time is $t_0 = 0$.

As $k(s) = 1$, the Hurwitz polynomial $f(s)$ in (4.16) can be chosen as $f(s) = (s+\lambda)^2$. Then, we have

$$\dot{y}(t) + \lambda y(t) = \frac{2\lambda s + \lambda^2}{s+\lambda} y(t) + \frac{1}{s+\lambda} v(t) \tag{4.40}$$

From Theorem 4.2, we construct the following two equations

$$\dot{\hat{y}}(t) + \lambda \hat{y}(t) = \left\{ \frac{2\lambda s + \lambda^2}{s+\lambda} y(t) + \frac{\mu_0}{s+\lambda} u(t) \right\} + w_1(t), \quad \hat{y}(0) = 0 \tag{4.41}$$

$$\dot{\hat{w}}_1(t) + \lambda \hat{w}_1(t) = w_2(t), \quad \hat{w}_1(0) = 0 \tag{4.42}$$

where $w_1(t)$ and $w_2(t)$ are determined by

$$w_1(t) = \frac{\left\{ \frac{1}{s+\lambda} \rho(t) \right\}^2 \{ y(t) - \hat{y}(t) \}}{\left\{ \frac{1}{s+\lambda} \rho(t) \right\} |y(t) - \hat{y}(t)| + \delta_1} \tag{4.43}$$

and

$$w_2(t) = \frac{\rho^2(t) \{ w_1(t) - \hat{w}_1(t) \}}{\rho(t) |w_1(t) - \hat{w}_1(t)| + \delta_2} \tag{4.44}$$

respectively. So, $w_1(t)$ and $w_2(t)$ can be regarded as the approximate estimates of $\frac{1}{s+\lambda} v(t)$ and $v(t)$, respectively.

In the simulation process, the sampling period is chosen as 1×10^{-4} second.

1) Characteristics of δ_i, λ and $\rho(t)$

For the disturbance $v(t) = \begin{cases} 0 & t \le 0.02 \\ 1 & t > 0.02 \end{cases}$ (suppose its bound is known as $\rho(t) = 2$), Figure 4.3 (with the condition $y(0) = 0$, λ is chosen as $\lambda = 16$) shows the differences between the real disturbance and their estimates by using different parameters δ_i $(i = 1, 2)$. It can be seen that the parameters δ_i

determines the estimating precision.

Remark 4.8 In order to get good estimates of the disturbances, the parameters δ_i in the new observer should be chosen to be very small. When the analog signals are implemented by a digital computer, the parameters δ_i should not be chosen to be much smaller than $T \cdot \max_{t_1 \ge t \ge t_0} \{ \omega_{r-1}(t) \}$, where T is the sampling period, t_1 is the ending time and $\omega_{r-1}(t)$ is defined in (4.14). Otherwise, as the variations of the functions $w_i(t)$ defined in (4.36) and (4.37) will be too fast with respect to the sampling frequency, Equations (4.34) and (4.35) can not be precisely solved.

Remark 4.9 Remark 4.8 also tells us that the new observer has some limitations for high frequency disturbances and large amplitude disturbances if the digital computer is employed.

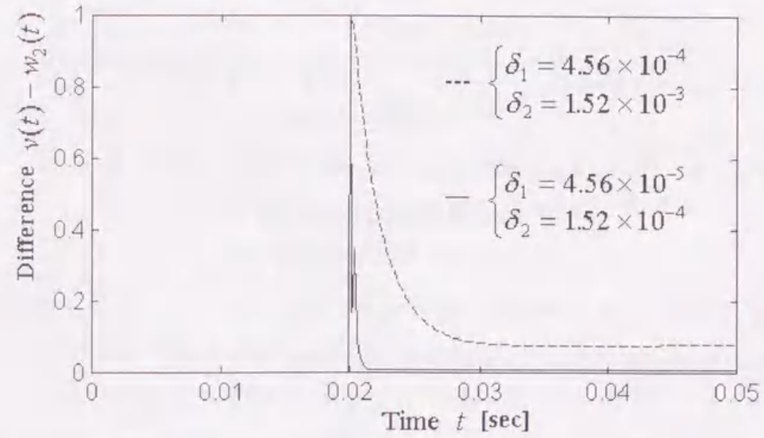

Fig. 4.3 The differences between the step disturbance and its estimates by using different parameters δ_i.

For the disturbance $v(t) = 1$ (suppose its bound is known as $\rho(t) = 2$), Figure 4.4 shows the differences between the real disturbance and its estimates by using

different parameters λ (with the condition $y(0)=0.1$, $\delta_1=\frac{2.28}{\lambda}\times 10^{-4}$ and $\delta_2=3.8\times 10^{-4}$). It can be seen that the parameter λ determines the estimating speed and precision. When the parameter λ is chosen to be too large, the estimating error will be large even though the parameters δ_i are chosen to be very small.

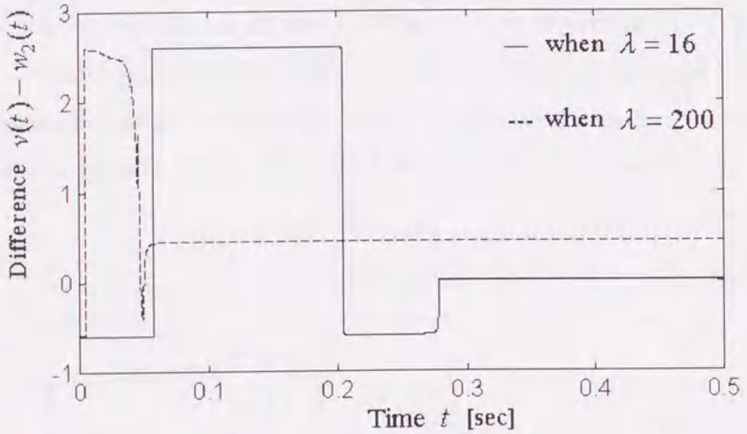

Fig. 4.4 The differences between the real disturbance and its estimates by using different parameters λ.

Remark 4.10 For a controlled system, the parameters λ and δ_i should be appropriately chosen to meet the particular requirement.

For the disturbance $v(t)=t$, Figure 4.5 (with the initial condition $y(0)=0$ and the choices $\lambda=16$, $\delta_1=8\times 10^{-5}$, $\delta_2=10^{-4}$) shows the simulation results of the differences between the disturbance and its estimates for different $\rho(t)$.

Remark 4.11 Figure 4.5 shows that $\rho(t)$ also influences the estimating speed. For definite parameters δ_i, appropriate large $\rho(t)$ can result in a good estimation.

The proofs of Relations (A62) and (A69) also imply this fact. But in the practical applications, $\rho(t)$ can not be very large due to the energy limitation. Moreover, by referring Remark 4.8, a very large $\rho(t)$ may result in a bad estimation when the signals are implemented by a digital computer (since the parameters δ_i should be chosen large for a definite sampling frequency). Thus, an appropriate *a priori* knowledge $\rho(t)$ is necessary to get a good estimation.

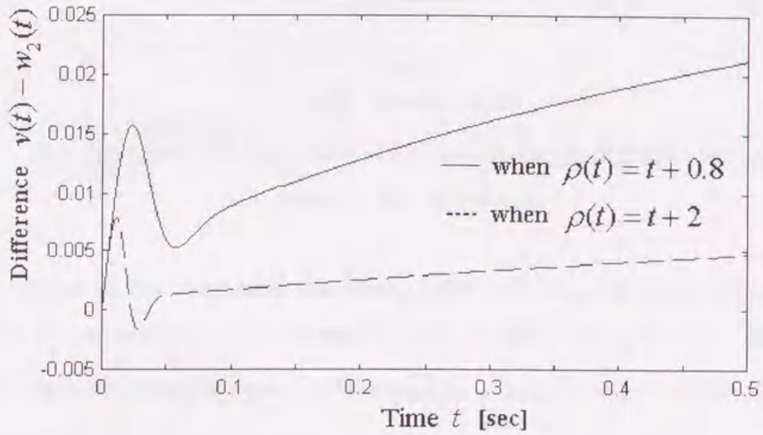

Fig. 4.5 The simulation results of the differences between the disturbance $v(t)=t$ and its estimates for different $\rho(t)$.

2) Ability of Observing Complicated Disturbances

Suppose $y(0)=0$ and the imposed disturbance is described by

$$v(t)=0.5\sin 100t+\phi(t)+\varphi(t)-y(t)+\frac{0.5y^2(t)\dot{y}(t)}{|\dot{y}(t)|+0.5} \tag{4.45}$$

where $\phi(t)=\begin{cases}0 & t\le 0.02\\ 0.5 & t>0.02\end{cases}$ and $\varphi(t)=\begin{cases}t & t\le 0.1\\ t^2 & t>0.1\end{cases}$. It can be seen that the disturbance $v(t)$ is composed of various kinds of disturbances. Suppose the upper bound of $|v(t)|$ is known as $\rho(t)=3.2$.

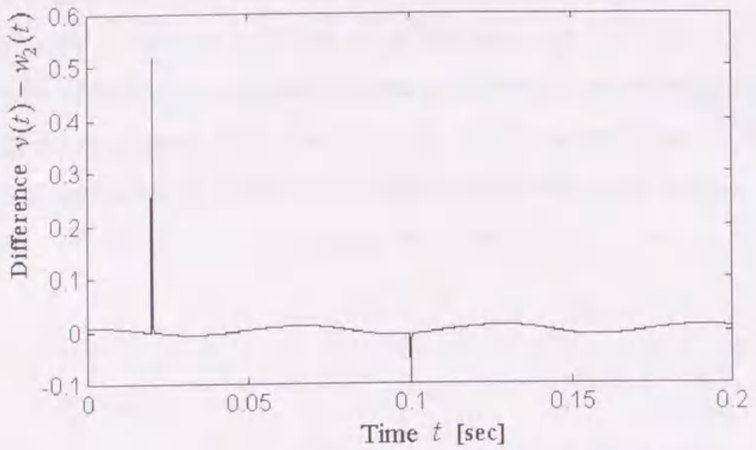

Fig. 4.6 The difference between the disturbance (4.45) and its estimate by using the new observer.

Figure 4.6 shows the difference between the real disturbance and its estimate by using the new observer where the parameters are chosen as $\lambda = 16$, $\delta_1 = 2.28 \times 10^{-4}$, $\delta_2 = 3.8 \times 10^{-4}$. To get a similar good estimation, the traditional observer should be chosen as $\frac{g_2 s^2}{s^2 + g_1 s + g_2} y(t)$, where $g_1 = 2 \times 10^4$ and $g_2 = 10^8$.

3) Performance in the Presence of Measurement Noises

As only the measurement of the output is employed in our formulation, corresponding to Equation (4.1), we just consider the system with output measurement noise (Gaussian white noises). Suppose the measured output is

$$Y(t) = y(t) + g(t) \tag{4.46}$$

where $y(t)$ is the genuine system output, $g(t)$ is a Gaussian white noises with the amplitude 4×10^{-7}. Under this assumption, the signal $y(t)$ in the formulation (4.41)-(4.44) should be replaced by $Y(t)$.

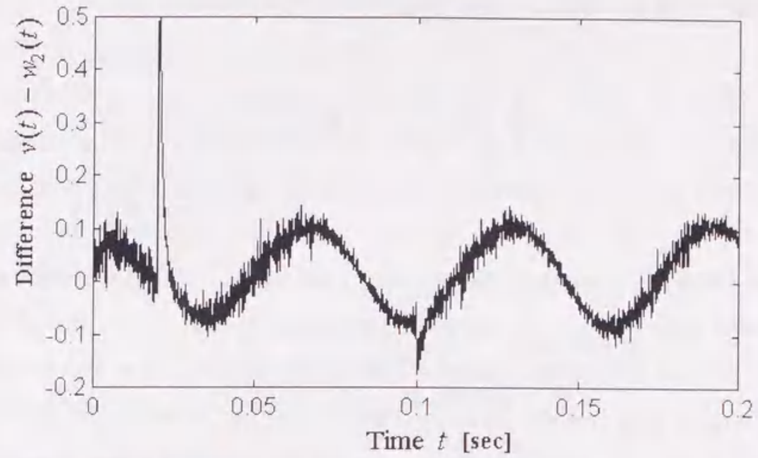

Fig. 4.7 The difference between the disturbance (4.45) and its estimate in the presence of measurement noises.

Suppose the disturbance is same as (4.45). In the presence of measurement noises, in order to get good estimates, the parameters δ_i should be chosen as $\delta_1 = 2.28 \times 10^{-3}$, $\delta_2 = 4.56 \times 10^{-3}$ in the new observer (when $\lambda = 16$), while the parameters g_i in the traditional observer should be chosen as $g_1 = 2 \times 10^3$, $g_2 = 10^6$ (the response is same as the new observer). The simulation result is shown in Figure 4.7.

Remark 4.12 In the presence of measurement noises, the parameters δ_i in the new observer should be chosen to be much larger, while the parameters g_i in the traditional observer should be chosen to be much smaller when comparing to the case in which the measurement noises are absent.

Remark 4.13 For a strictly proper system, we do not consider the case when a very high frequency noise is accompanied with the input or involved in the disturbance because the influence over the output of this kind noise is very small and can be omitted.

4.6 Extension to a Class of Nonminimum Phase Dynamical Systems

In this section, we consider the case when the real parts of the roots of $k(s)$ are smaller than 1, i.e. the system (4.1) may be in nonminimum phase. About estimating the disturbance for the nonminimum phase systems, no results has been reported until now.

In the following, inspired by the techniques introduced in [62] for discrete-time nonminimum phase systems, we derive the approximate inverse systems for the class of continuous-time nonminimum phase systems in which the real parts of the roots of $k(s)$ are smaller than 1, where the approximation error can be made as small as it is needed. Based on the obtained approximate inverse system, a robust disturbance observer is formulated for the nonminimum phase dynamical systems with arbitrarily relative degrees.

4.6.1 Approximate Inverse Systems

Suppose $k_r \neq 0$ and $k_i = 0$ for $i \leq r-1$. Now, we express $k(s)$ as

$$k(s) = k_r \kappa_1(s)\kappa_2(s), \tag{4.47}$$

where $\kappa_1(s)$ is a υ-th order monic polynomial with no root lying in the left half plane, $\kappa_2(s)$ is an $(n-r-\upsilon)$-th order monic Hurwitz polynomial. Further, we suppose

$$\kappa_1(s) = (s-\eta_1)\cdots(s-\eta_\tau)(s-\alpha_1)(s-\overline{\alpha}_1)\cdots(s-\alpha_\iota)(s-\overline{\alpha}_\iota), \tag{4.48}$$

where η_i $(i=1,\cdots,\tau)$ are real numbers satisfying $1 > \eta_i \geq 0$; α_j $(j=1,\cdots,\iota)$ are complex numbers satisfying $1 > \mathrm{Re}(\alpha_j) \geq 0$; $\tau + 2\iota = \upsilon$.

Now, we introduce the next polynomial

$$\xi(s) = \left\{\left\{\prod_{i=1}^{\tau}(s+\chi_i)\right\}\left\{\prod_{j=1}^{\iota}(s+\beta_j)(s+\overline{\beta}_j)\right\}\right\}^{\gamma+1}, \tag{4.49}$$

where γ is a positive integer, χ_i $(i=1,\cdots,\tau)$ are positive real numbers, β_j $(j=1,\cdots,\iota)$ are complex numbers. Let

$$(s+\chi_i)^{\gamma+1} = s^{\gamma+1} + g_{i1}s^{\gamma} + \cdots + g_{i\gamma}s + g_{i,\gamma+1}, \quad i=1,\cdots,\tau, \tag{4.50}$$

$$(s+\beta_j)^{\gamma+1} = s^{\gamma+1} + l_{j1}s^{\gamma} + \cdots + l_{j\gamma}s + l_{j,\gamma+1}, \quad j=1,\cdots,\iota. \tag{4.51}$$

Further, we introduce the following polynomials

$$\theta_i(s) = s^{\gamma} + \theta_{i1}s^{\gamma-1} + \cdots + \theta_{i,\gamma-1}s + \theta_{i\gamma}, \quad i=1,\cdots,\tau, \tag{4.52}$$

$$\vartheta_j(s) = s^{\gamma} + \vartheta_{j1}s^{\gamma-1} + \cdots + \vartheta_{j,\gamma-1}s + \vartheta_{j\gamma}, \quad j=1,\cdots,\iota. \tag{4.53}$$

The coefficients of $\theta_i(s)$ and $\vartheta_j(s)$ are described by

$$\theta_i = (N_i^T N_i)^{-1} N_i^T g_i, \quad \vartheta_j = (K_j^* K_j)^{-1} N_j^* l_j, \tag{4.54}$$

where

$$N_i = \begin{bmatrix} 1 & 0 & \cdots & 0 \\ -\eta_i & 1 & \cdots & \vdots \\ 0 & -\eta_i & \ddots & 0 \\ \vdots & \vdots & \ddots & \vdots \\ 0 & 0 & \cdots & 1 \\ 0 & 0 & \cdots & -\eta_i \end{bmatrix}, \quad \theta_i = \begin{bmatrix} 1 \\ \theta_{i1} \\ \vdots \\ \theta_{i\gamma} \end{bmatrix}, \quad g_i = \begin{bmatrix} 1 \\ g_{i1} \\ \vdots \\ g_{i,\gamma+1} \end{bmatrix}, \tag{4.55}$$

$$K_j = \begin{bmatrix} 1 & 0 & \cdots & 0 \\ -\alpha_j & 1 & \cdots & \vdots \\ 0 & -\alpha_j & \ddots & 0 \\ \vdots & \vdots & \ddots & \vdots \\ 0 & 0 & \cdots & 1 \\ 0 & 0 & \cdots & -\alpha_j \end{bmatrix}, \quad \vartheta_j = \begin{bmatrix} 1 \\ \vartheta_{j1} \\ \vdots \\ \vartheta_{j\gamma} \end{bmatrix}, \quad l_j = \begin{bmatrix} 1 \\ l_{j1} \\ \vdots \\ l_{j,\gamma+1} \end{bmatrix}, \tag{4.56}$$

for $i=1,\cdots,\tau$, $j=1,\cdots,\iota$. Define

$$\varsigma(s) = \left\{\prod_{i=1}^{\tau}\theta_i(s)\right\}\left\{\prod_{j=1}^{\iota}\vartheta_j(s)\overline{\vartheta}_j(s)\right\}. \tag{4.57}$$

The next theorem gives the approximate inverse system of $\kappa_1(s)$.

Theorem 4.3 If the parameters χ_i $(i=1,\cdots,\tau)$ and β_j $(j=1,\cdots,\iota)$ are chosen

such that $1-\eta_i > \chi_i > 0$, $0 < \mathrm{Re}(\beta_j) < 1 - \mathrm{Re}(\alpha_j)$, $\mathrm{Im}(\beta_j) = -\mathrm{Im}(\alpha_j)$, then $\kappa_1(s)$ can be approximated by $\dfrac{\xi(s)}{\varsigma(s)}$ as $\gamma \to \infty$.

Proof: See A.8 in the Appendix .

Remark 4.14 It should be pointed out that $\xi(s)$ is a $(\gamma+1)\upsilon$-*th* order monic Hurwitz polynomial with real coefficients, and $\varsigma(s)$ is a $\gamma\upsilon$-*th* order monic polynomial with real coefficients.

4.6.2 Identification of the Disturbance

Define

$$\bar{v}(t) = \frac{\kappa_1(s)\varsigma(s)}{\xi(s)} v(t) \tag{4.58}$$

Equation (1) can be rewritten as

$$a(s)\varsigma(s)y(t) = b(s)\varsigma(s)u(t) + k_r\kappa_2(s)\xi(s)\bar{v}(t), \tag{4.59}$$

where $a(s)\varsigma(s)$ is a monic $(n+\upsilon p)$-th order polynomial, $b(s)\varsigma(s)$ is a polynomial with at most $(n+\upsilon p-1)$-th order, $\kappa_2(s)\xi(s)$ is a monic $(n+\upsilon p-r)$-th order Hurwitz polynomial.

Theorem 4.3 also tells us that $v(t)-\bar{v}(t) \to 0$ as $\gamma \to \infty$, for all t. Thus, the estimation of $\bar{v}(t)$ can be approximately regarded as the estimation of $v(t)$ as γ is large enough. On the other hand, from Theorem 4.2, it can be seen that $\bar{v}(t)$ can be approximately estimated based on the minimum phase dynamical system (4.59) (with respect to the relation between $y(t)$ and $\bar{v}(t)$). First, the upper bound of $\bar{v}(t)$ must be estimated.

Lemma 4.3 For a small positive constant $\mu > 0$, there exists a positive integer Γ such that

$$|\bar{v}(t)| \le \rho(y,u,t) + \mu \tag{4.60}$$

for all $\gamma > \Gamma$.

Proof: The result is obvious by using Theorem 4.3.

Thus, the upper bound of $\left|\dfrac{1}{(s+\lambda)^t}\bar{v}(t)\right|$ can be estimated as

$$\left|\frac{1}{(s+\lambda)^t}\bar{v}(t)\right| \le \frac{1}{(s+\lambda)^t}\{\rho(y,u,t)+\mu\} \triangleq \bar{\omega}_t(t) \tag{4.61}$$

Remark 4.15 By the definition in (4.61), it is obvious that $\bar{\omega}_0(t) = \rho(y,u,t) + \mu$.

Therefore, based on Equation (4.59), by choosing the Hurwitz polynomial $f(s) = \kappa_2(s)\xi(s)(s+\lambda)^r$, the disturbance can be approximately estimated by the next theorem for the class of nonminimum phase dynamical systems.

Theorem 4.4 For the class of nonminimum phase dynamical systems described in this section, construct the dynamical systems described by

$$\dot{\hat{y}}(t) + \lambda\hat{y}(t) = \frac{f(s)-a(s)\varsigma(s)}{\kappa_2(s)\xi(s)(s+\lambda)^{r-1}}y(t) + \frac{b(s)\varsigma(s)}{\kappa_2(s)\xi(s)(s+\lambda)^{r-1}}u(t), + k_r w_1(t), \quad \hat{y}(t_0) = 0, \tag{4.62}$$

$$\dot{\hat{w}}_{i-1}(t) + \lambda\hat{w}_{i-1}(t) = w_i(t), \quad \hat{w}_{i-1}(t_0) = 0, \tag{4.63}$$

where $\varsigma(s)$ and $\xi(s)$ are given in Theorem 4.3, and, for small positive constants $\delta_i > 0$ $(i = 1,\cdots,r)$, $w_i(t)$ are given by

$$w_1(t) = \frac{k_r\bar{y}(t)\omega_{r-1}^2(t)}{|k_r\bar{y}(t)|\omega_{r-1}(t) + \delta_1}, \tag{4.64}$$

$$w_i(t) = \frac{\{w_{i-1}(t) - \hat{w}_{i-1}(t)\}\omega_{r-i}^2(t)}{|w_{i-1}(t) - \hat{w}_{i-1}(t)|\omega_{r-i}(t) + \delta_i} \quad (i = 2,\cdots,r) \tag{4.65}$$

respectively. Then, there exists $\varepsilon(\gamma,\delta_1,\cdots,\delta_r) > 0$ such that

$$|v(t) - w_r(t)| \le \varepsilon(\gamma,\delta_1,\cdots,\delta_r), \text{ as } t \to \infty \text{ and } \gamma > \Gamma, \tag{4.66}$$

where $\varepsilon(\gamma,\delta_1,\cdots,\delta_r) \to 0$ as $\gamma \to \infty$ and $\sum_{j=1}^{r}\delta_j \to 0$, i.e. $w_r(t)$ is the approximate estimate of $v(t)$.

Proof: The result can be easily obtained by employing Theorems 4.2 and 4.3.

The disturbance identification algorithm for a class of nonminimum phase dynamical systems with relative degree r is illustrated in Table 4.2.

Table 4.2 The algorithm of identifying the disturbance for a class of nonminimum phase dynamical systems with relative degree r

Plant	$a(s)y(t) = b(s)u(t) + k(s)v(x,u,t), \quad k(s) = k_r\kappa_1(s)\kappa_2(s)$ $\kappa_1(s) = (s-\eta_1)\cdots(s-\eta_\tau)(s-\alpha_1)(s-\overline{\alpha}_1)\cdots(s-\alpha_t)(s-\overline{\alpha}_t)$ $1 > \eta_i \geq 0, \ 1 > \mathrm{Re}(\alpha_j) \geq 0$ $\kappa_2(s)$: monic Hurwitz polynomial
A priori information	$\lvert v(x,u,t)\rvert \leq \rho(y,u,t)$
Approximate of $\kappa_1(s)$	$\kappa_1(s) = \dfrac{\xi(s)}{\varsigma(s)}$, as $\gamma \to \infty$ $\xi(s)$: monic Hurwitz polynomial
Transformed plant	$a(s)\varsigma(s)y(t) = b(s)\varsigma(s)u(t) + k_r\kappa_2(s)\xi(s)\bar{v}(t), \ \bar{v}(t) = \dfrac{\kappa_1(s)\varsigma(s)}{\xi(s)}v(t)$ (A minimum phase system with relative degree r)
Upper bound of $\bar{v}(t)$	$\lvert\bar{v}(t)\rvert \leq \rho(y,u,t) + \mu$ (Thus, $\left\lvert \dfrac{1}{(s+\lambda)^i}\bar{v}(t)\right\rvert \leq \dfrac{1}{(s+\lambda)^i}\{\rho(y,u,t)+\mu\} \triangleq \bar{\omega}_i(t)$)
Estimate of $\bar{v}(t)$	$w_r(t)$ (By employing the algorithm in 4.4)
Estimate of $v(t)$	Approximately $w_r(t)$ (Since $v(t) - \bar{v}(t) \to 0$ as $\gamma \to \infty$)

4.7 Application to a State Observer

In this section, the state observer is constructed by employing the estimate of the disturbance obtained in Theorems 4.2 and 4.4 even though the system is in nonminimum phase.

To begin with, we introduce a stable matrix defined by

$$G = \begin{bmatrix} -g_1 & 1 & 0 & \cdots & 0 \\ -g_2 & 0 & 1 & \cdots & 0 \\ \cdot & \cdot & \cdot & \cdots & \cdot \\ -g_{n-1} & 0 & 0 & \cdots & 1 \\ -g_n & 0 & 0 & \cdots & 0 \end{bmatrix} \triangleq \begin{bmatrix} I \\ -g \end{bmatrix}_0 \tag{4.67}$$

Now, consider the state observer of system (4.1) given by

$$\begin{cases} \dot{\hat{x}}(t) = A\hat{x}(t) + bu(t) + kw(t) + (g-a)(y(t) - \hat{y}_1(t)) \\ \hat{y}_1(t) = c^T\hat{x}(t) \end{cases} \tag{4.68}$$

where $\hat{x}(t)$ is the estimated state with the initial condition $\hat{x}(t_0) = 0$, $w(t)$ is the estimate of the disturbance $v(t)$ obtained from Theorem 4.2 or Theorem 4.4. Let

$$\bar{x}(t) = x(t) - \hat{x}(t) \tag{4.69}$$

be the state error. From (4.1) and (4.68),

$$\dot{\bar{x}}(t) = G\bar{x}(t) + k\{v(t) - w(t)\} \tag{4.70}$$

As $w(t)$ is an approximate estimate of $v(t)$, by employing the stability of G, it can be easily proved that $\bar{x}(t)$ is very small as $t \to \infty$. Thus, we get the next Theorem.

Theorem 4.5 The VSS type state observer of system (4.1) can be formulated as (4.68), where $w(t)$ is the estimate of the disturbance obtained from Theorem 4.2 if the system (4.1) is in minimum phase; otherwise, $w(t)$ is obtained from Theorem 4.4.

The block diagram of the state observer employing the disturbance identification of the uncertain system (4.1) is shown in Figure 4.8.

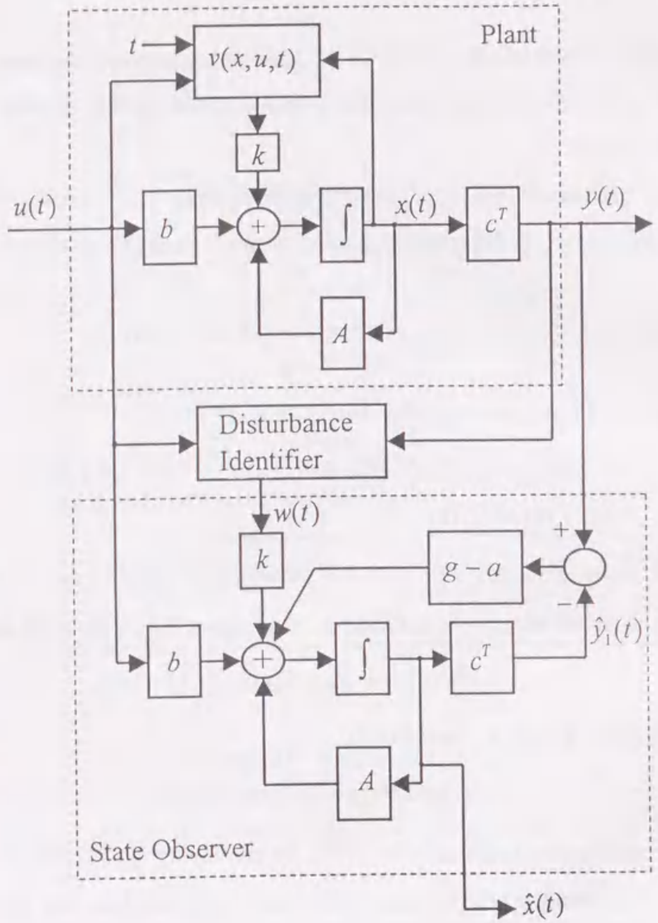

Fig. 4.8 The block diagram of the state observer of the unknown system (4.1).

4.8 Application to a Pole Assignment Controller

In this section, we assume that the disturbance is matched, i.e. $b = k$. We also assume that the *a priori* function $\rho(y(t), u(t), t)$ has no relation with the input $u(t)$.

Let the desired closed-loop transfer function be represented by

$$G_d(s) = \frac{b(s)}{d(s)} \tag{4.71}$$

where the zeros of the Hurwitz denominator polynomial

$$d(s) = s^n + d_1 s^{n-1} + \cdots + d_n \tag{4.72}$$

determine the zeros of the desired closed-loop poles.

Consider a linear state feedback control law defined by

$$u(t) = -\kappa^T \hat{x}(t) - w(t) + \psi(t) \tag{4.73}$$

where κ is an $n \times 1$ feedback gain vector, $\hat{x}(t)$ is the estimated state obtained in (4.68), $\psi(t)$ is a uniformly bounded external input and $w(t)$ is the estimate of the disturbance $v(t)$ employed to cancel $v(t)$. With an appropriate choice of the feedback gain vector κ, the characteristic equation of the closed-loop system becomes

$$\det(sI - A + b\kappa^T) = d(s) \tag{4.74}$$

One method of calculating the feedback gain κ can be found in [36].

The block diagram of controlled closed loop system is shown in Figure 4.9.

Now, applying the control law described in (4.73) to (4.1) yields

$$\dot{x}(t) = (A - b\kappa^T)x(t) + b\psi(t) + b\kappa^T \bar{x}(t) + b\{v(t) - w(t)\} \tag{4.75}$$

As $A - b\kappa^T$ is a stable matrix, from (4.75), it can be concluded that $x(t)$ is uniformly bounded by using Theorems 4.2-4.5 and the facts that $\psi(t)$ is a uniformly bounded signal. Further, from (4.73), we can also concluded that $u(t)$ is uniformly bounded.

Therefore, (4.75) gives

$$y(t) = \frac{b(s)}{d(s)}\gamma(t) + \frac{b(s)}{d(s)}\{\kappa^T \bar{x}(t) + v(t) - w(t)\} \tag{4.76}$$

Let $y_d(t) \triangleq \dfrac{b(s)}{d(s)}\psi(t)$. (4.76) can written as

$$y(t) - y_d(t) = \frac{b(s)}{d(s)}\{\kappa^T \bar{x}(t) + v(t) - w(t)\} \tag{4.77}$$

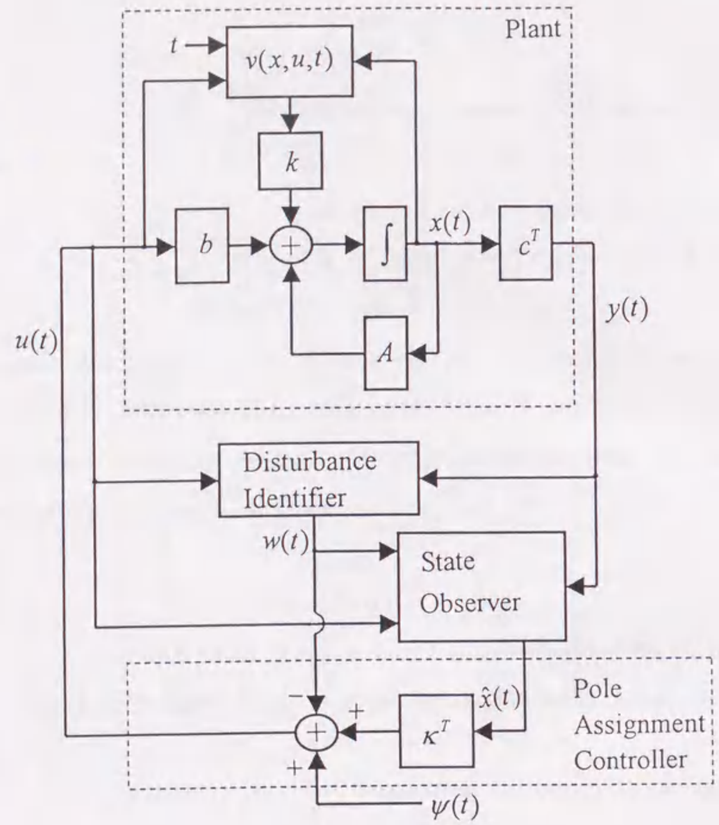

Fig. 4.9 The block diagram of the pole assignment control system.

Since $\bar{x}(t)$ and $v(t)-w(t)$ are very small as $t\to\infty$, by using that $d(s)$ is a Hurwitz polynomial, it can be easily concluded that $y(t)-y_d(t)$ is very small as $t\to\infty$, i.e. the pole assignment can be approximately achieved as $t\to\infty$. Therefore, the next theorem is obtained.

Theorem 4.6 With the pole assignment controller (4.73), where $\hat{x}(t)$ is characterized by (4.68) and the signal $w(t)$ is the estimate of the disturbance generated from Theorem 4.2 or Theorem 4.4, the overall system is uniformly bounded and the output $y(t)$ approximately tracks the desired output $y_d(t)=\dfrac{b(s)}{d(s)}\psi(t)$ as

$t\to\infty$.

The pole assignment control algorithm is illustrated in Table 4.3.

Table 4.3 The algorithm of the pole assignment control

Plant	$a(s)y(t)=b(s)u(t)+k(s)v(x,u,t)$, (The real parts of the roots of $k(s)$ are smaller than 1)
A priori information	$\lvert v(x,u,t)\rvert\le\rho(y,u,t)$
Desired poles	The roots of the Hurwitz polynomial $d(s)=s^n+d_1s^{n-1}+\cdots+d_n$
Identified disturbance	$w(t)$ (By the algorithm presented in Table 4.1 or Table 4.2)
State observer	$\begin{cases}\dot{\hat{x}}(t)=A\hat{x}(t)+bu(t)+kw(t)+(g-a)(y(t)-\hat{y}_1(t))\\ \hat{y}_1(t)=c^T\hat{x}(t)\end{cases}$
Feedback gain	κ
External input	$\psi(t)$ (a uniformly bounded signal)
Pole assignment controller	$u(t)=-\kappa^T\hat{x}(t)-w(t)+\psi(t)$

4.9 Design Example and the Simulation Results

In this section, a nonminimum phase system will be presented to show the design procedure of the proposed nonlinear disturbance observer, state observer and the pole assignment controller.

Example Consider the unstable system described by

$$\begin{cases} \dot{x}(t) = \begin{bmatrix} 3 & 1 & 0 \\ -3 & 0 & 1 \\ 1 & 0 & 0 \end{bmatrix} x(t) + \begin{bmatrix} 0 \\ 4 \\ -0.5 \end{bmatrix} (u(t) + v(t)) \\ y(t) = [1,0,0] x(t) = x_1(t) \end{cases} \tag{4.78}$$

where $y(t)$ is the output; $u(t)$ is the input; $v(t)$ is the unknown disturbance described by

$$v(t) = \cos(5t) \frac{y(t)(\dot{y}(t) + u(t))}{|\dot{y}(t) + u(t)| + 0.5} \tag{4.79}$$

Suppose the upper bound of $v(t)$ is known as $|v(t)| \le \rho(y,u,t) = 1.5|y(t)|$. The starting time is $t_0 = 0$. For simplicity, the unknown initial condition of the state is assumed as $x(0) = 0$.

The closed-loop poles are desired as the roots of the polynomial

$$d(s) = s^3 + 6s^2 + 12s + 8 \tag{4.80}$$

The external reference input is chosen to be

$$\psi(t) = 2\sin t \tag{4.81}$$

Then, the feedback gain κ can be calculated as

$$\kappa = [9.3406,\ 2.7287,\ 3.8309]^T \tag{4.82}$$

As $k(s) = 4(s - 0.125)$ is a first order polynomial, for simplicity, we use the inverse system formulation proposed for $s - \alpha$ in the Appendix (A83)-(A89). The parameter β is chosen as $\beta = 0.3$. The accuracy of the approximate inverse system depends on the choice of the parameter γ. However, when γ is chosen too large, the computation may become complicated. In the presented examples, γ is chosen as $\gamma = 7$. Under the above choice, the value of J (see (A89) in the Appendix) is $J = 1.1153 \times 10^{-6}$. The least-square approximate solution c of Equation (A87) is obtained as

$$c_1 = 2.5250,\ c_2 = 2.8356,\ c_3 = 1.8665,\ c_4 = 0.8003, \tag{4.83}$$

$$c_5 = 0.2369,\ c_6 = 0.0499,\ c_7 = 0.0079. \tag{4.84}$$

Choose the Hurwitz polynomial $f(s)$ in Theorem 4.4 as

$$f(s) = (s + 0.3)^8 (s + 2)^2, \tag{4.85}$$

where λ is chosen as $\lambda = 2$. From (4.78), we have

$$\dot{y}(t) + 2y(t) = \frac{f(s) - (s+1)^3 q(s)}{(s+0.3)^8 (s+2)} y(t) + \frac{(2s-1)q(s)}{(s+0.3)^8 (s+2)} u(t) + \frac{4}{(s+2)} \bar{v}(t), \tag{4.86}$$

$$\bar{v}(t) = \frac{(s - 0.125)q(s)}{(s+0.3)^8} v(t). \tag{4.87}$$

From Theorem 3, we construct the following dynamical systems

$$\dot{\hat{y}}(t) + 2\hat{y}(t) = \frac{f(s) - (s+1)^3 q(s)}{(s+0.3)^8 (s+2)} y(t) + \frac{(2s-1)q(s)}{(s+0.3)^8 (s+2)} u(t) + 4w_1(t), \tag{4.88}$$

$$\dot{\hat{w}}_1(t) + 2\hat{w}_1(t) = w_2(t), \tag{4.89}$$

where $\hat{y}(0) = 0$, $\hat{w}_1(0) = 0$, $w_1(t)$ and $w_2(t)$ are determined by

$$w_1(t) = \frac{4\{y(t) - \hat{y}(t)\} \left\{ \frac{1}{s+2} \left(1.5|y(t)| + \mu\right) \right\}^2}{4|y(t) - \hat{y}(t)| \left\{ \frac{1}{s+2} \left(1.5|y(t)| + \mu\right) \right\} + \delta_1}, \tag{4.90}$$

and

$$w_2(t) = \frac{\{w_1(t) - \hat{w}_1(t)\} \{1.5|y(t)| + \mu\}^2}{|w_1(t) - \hat{w}_1(t)| \{1.5|y(t)| + \mu\} + \delta_2}, \tag{4.91}$$

respectively. Therefore, $w_2(t)$ can be regarded as the approximate estimate of the disturbance $v(t)$.

The state observer is constructed as

$$\begin{cases} \dot{\hat{x}}(t) = \begin{bmatrix} 3 & 1 & 0 \\ -3 & 0 & 1 \\ 1 & 0 & 0 \end{bmatrix} \hat{x}(t) + \begin{bmatrix} 0 \\ 4 \\ -0.5 \end{bmatrix} \{u(t) + w_2(t)\} + \left\{ \begin{bmatrix} 3 \\ 3 \\ 1 \end{bmatrix} - \begin{bmatrix} -3 \\ 3 \\ -1 \end{bmatrix} \right\} \{y(t) - \hat{y}_1(t)\} \\ \hat{y}_1(t) = [1,0,0] x(t) = \hat{x}_1(t) \end{cases} \tag{4.92}$$

where the vector g in (4.67) is chosen as $g = [3, 3, 1]^T$.

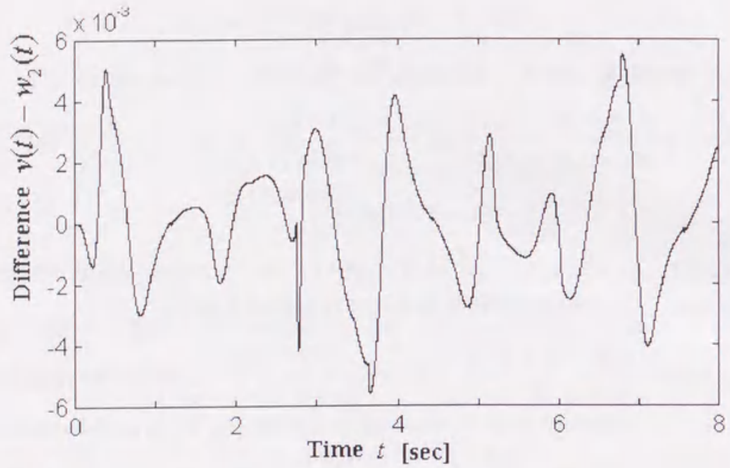

Fig. 4.10 The difference between the disturbance $v(t)$ and its estimate $w_2(t)$.

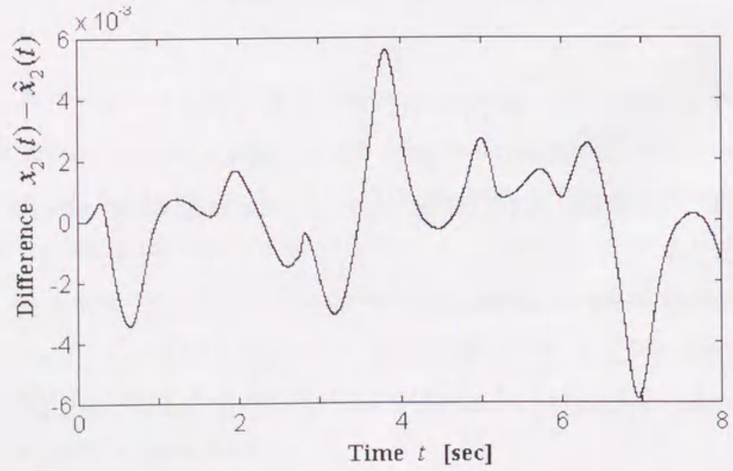

Fig. 4.11 The difference between the state $x_2(t)$ and its estimate $\hat{x}_2(t)$.

The pole placement controller is synthesized as

$$u(t) = -\kappa\hat{x}(t) - w_2(t) + \psi(t) \tag{4.93}$$

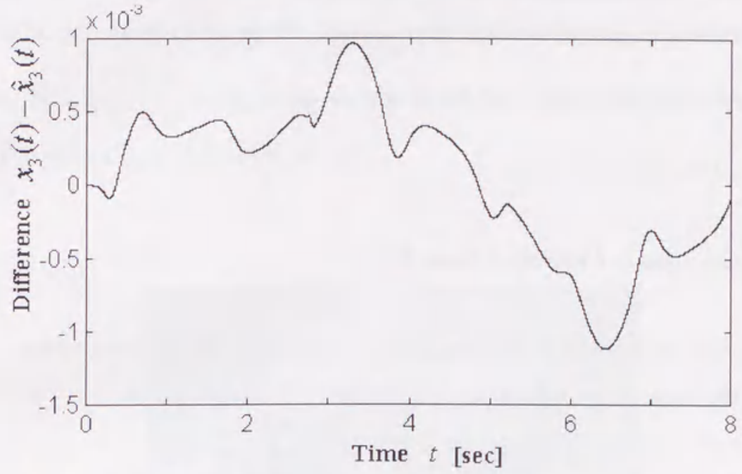

Fig. 4.12 The difference between the state $x_3(t)$ and its estimate $\hat{x}_3(t)$.

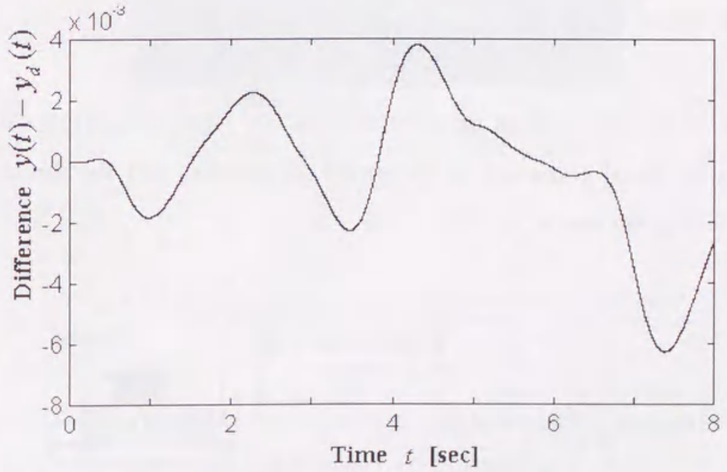

Fig. 4.13 The difference between the controlled output $y(t)$ and the desired output $y_d(t)$.

In the presented computer simulation process, μ is set to 0.2, δ_i is chosen as $\delta_1 = \delta_2 = 0.01$ and the sampling period is chosen as 0.01 second. The simulation results of the estimated disturbance and the state are shown in Figures 4.10-4.12. It can be seen that very good estimates are obtained. Figure 4.13 shows the difference between the controlled output and the desired signal $y_d(t) = \dfrac{4s-0.5}{(s+2)^3} 2\sin t$, where a very good tracking is achieved.

4.10 Application to Control a Linear Motor

In this section, the new disturbance observer is applied to control a linear motor. The model of the linear motor can be described by the following equation

$$s^2 y(t) = \mu_t u(t) + \kappa_t \hat{v}(t) \tag{4.94}$$

where $y(t)$ is the position; $u(t)$ is the control input (current); $\hat{v}(t)$ is the unknown term composed of the model uncertainties, the friction forces, the interaction forces, etc.; μ_t and κ_t are the unknown time varying parameters. Now, we rewrite system (4.94) as

$$s^2 y(t) = \mu_0 u(t) + v(t) \tag{4.95}$$

where μ_0 is the parameter of the nominal plant, $v(t) = (\mu_t - \mu_0)u(t) + \kappa_t \hat{v}(t)$ is the unknown signal composed of the model uncertainties and the disturbances. Suppose the starting time is $t_0 = 0$.

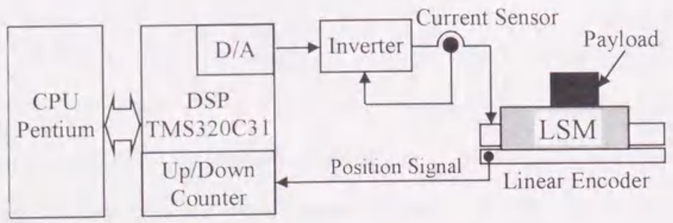

Fig. 4.14 The experimental system for the linear motor.

The experiment system is shown in Figure 4.14. Figure 4.15 is the picture of the experimental equipment. Figure 4.16 shows the linear motor. The specifications of the linear motor is shown in Table 4.4. Thus, the parameter μ_0 of the nominal model is calculated as $\mu_0 = 43/(3.3 \times 9.5) \approx 1.37$. For this linear motor, the upper bound of $|v(t)|$ is known as $|v(t)| \le 7.6$. The control purpose is to force the output $y(t)$ to track a desired position $y_m(t)$.

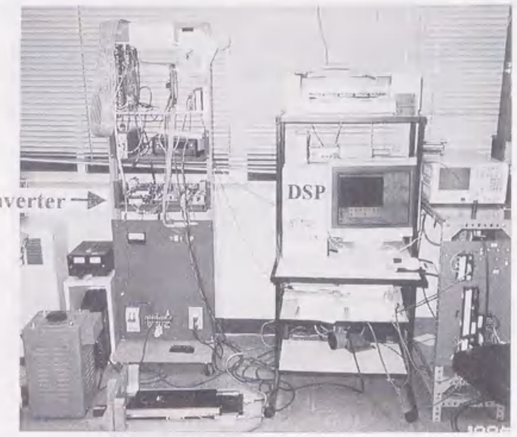

Linear Motor

Fig. 4.15 The experimental equipment of the linear motor.

As $k(s) = 1$, the Hurwitz polynomial $f(s)$ in (4.16) can be chosen as $f(s) = (s+\lambda)^2$. Then, we have

$$\dot{y}(t) + \lambda y(t) = \frac{2\lambda s + \lambda^2}{s+\lambda} y(t) + \frac{1.37}{s+\lambda} u(t) + \frac{1}{s+\lambda} v(t) \tag{4.96}$$

Table 4.4 Specification of the linear motor

Rated thrust	43 [N]
Rated current	3.3 [A]
Table mass	9.5 [kg]
Maximum speed	104 [cm/s]
Resolution of linear encoder	0.5 [μm]

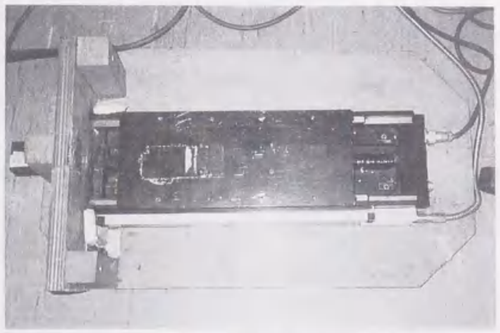

Fig. 4.16 The linear motor.

From Theorem 4.2, we construct the following two equations

$$\dot{\hat{y}}(t) + \lambda\hat{y}(t) = \left\{\frac{2\lambda s + \lambda^2}{s+\lambda}y(t) + \frac{1.37}{s+\lambda}u(t)\right\} + w_1(t), \quad \hat{y}(0) = 0 \tag{4.97}$$

$$\dot{\hat{w}}_1(t) + \lambda\hat{w}_1(t) = w_2(t), \quad \hat{w}(0) = 0 \tag{4.98}$$

where $w_1(t)$ and $w_2(t)$ are determined as

$$w_1(t) = \frac{\left\{\dfrac{1}{s+\lambda}7.6\right\}^2\{y(t) - \hat{y}(t)\}}{\left\{\dfrac{1}{s+\lambda}7.6\right\}|y(t) - \hat{y}(t)| + \delta_1} \tag{4.99}$$

and

$$w_2(t) = \frac{7.6^2\{w_1(t) - \hat{w}_1(t)\}}{7.6|w_1(t) - \hat{w}_1(t)| + \delta_2} \tag{4.100}$$

respectively. So, $w_1(t)$ and $w_2(t)$ can be regarded as the approximate estimates of $\dfrac{1}{s+\lambda}v(t)$ and $v(t)$, respectively.

The control $u(t)$ is determined as

$$u(t) = \frac{1}{1.37}\left\{s^2 y_m(t) + 200\{sy_m(t) - s\hat{y}(t)\} + 10000\{y_m(t) - y(t)\}\right\} - w_2(t) \tag{4.101}$$

where $w_2(t)$ is the estimated disturbance used to cancel the disturbance $v(t)$, $s\hat{y}(t)$ is the estimated speed. The poles of the position controller are set to $(-100 \pm j0)$ rad/sec. The sampling period is 1×10^{-4} second.

From Theorem 1, it can be seen that the speed observer can be formulated as

$$s\hat{y}(t) = -\lambda'\hat{y}(t) + \frac{2\lambda's + \lambda'^2}{s+\lambda'}y(t) + \frac{1.37}{s+\lambda'}u(t) + \frac{\left\{\dfrac{1}{s+\lambda'}7.6\right\}^2\{y(t) - \hat{y}(t)\}}{\left\{\dfrac{1}{s+\lambda'}7.6\right\}|y(t) - \hat{y}(t)| + \delta_1'} \tag{4.102}$$

By using the controller (4.101), the best performance of the controlled motor using the new observer is very similar to that using the traditional observer, where the parameters in the new disturbance observer and the new speed observer are chosen as $\lambda = 5$, $\delta_1 = 6\times10^{-4}$, $\delta_2 = 2\times10^{-4}$, $\lambda' = 10$ and $\delta_1' = 3.5\times10^{-4}$, while the traditional disturbance observer and traditional speed observer are designed as $w_2(t) = \dfrac{10^6}{s^2 + 2\times10^3 s + 10^6}s^2 y(t) - 1.37u(t)$ and $s\hat{y}(t) = \dfrac{10^3}{s+10^3}sy(t)$, respectively. Figure 4.17 shows the best performance of the motor controlled by (4.101). The signal in the top is the desired position $y_m(t)$ (2 [cm]/div). The second signal from the top is the tracking error (6.25×10^{-4} [cm]/div). The third

signal from the top shows the estimated speed $s\hat{y}(t)$ (5[cm/s]/div). The signal in the bottom is the observed disturbance (10[cm/s^2]/div).

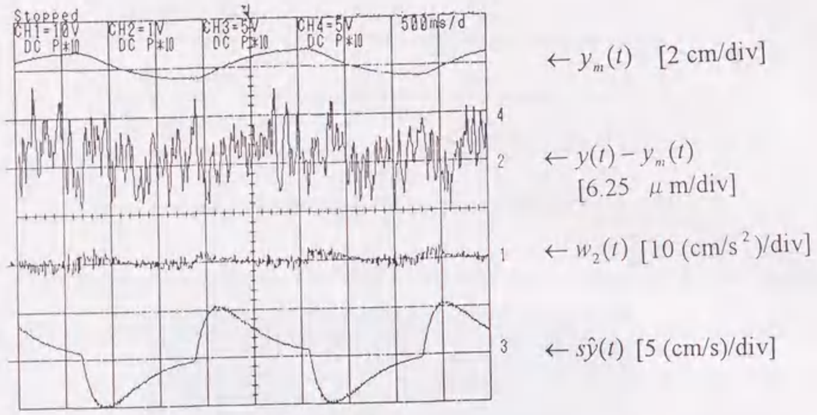

Fig. 4. 17 The best performance of the motor controlled by (4.101).

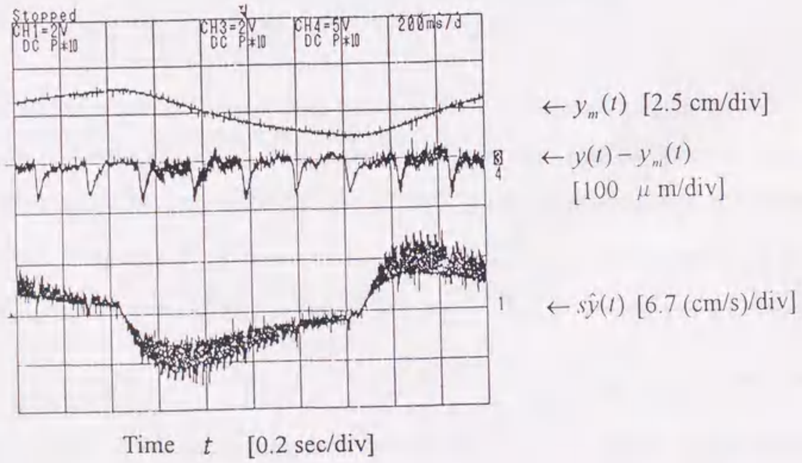

Fig. 4.18 Experimental results of the position controlled linear motor by using the new observers when the impulse disturbance is added.

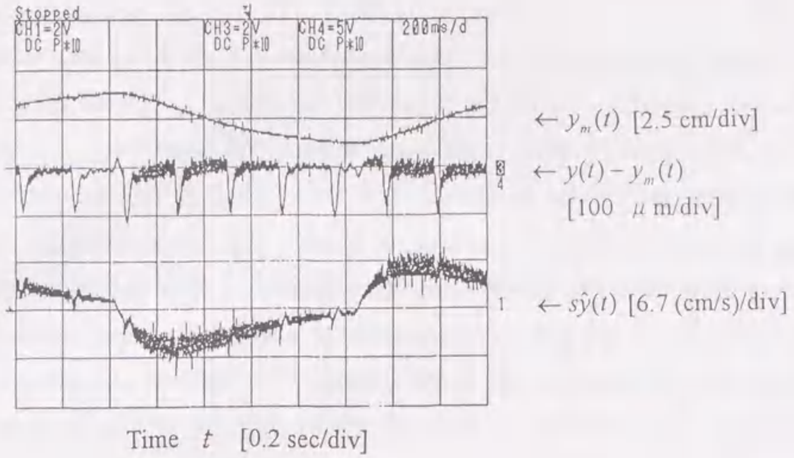

Fig. 4.19 Experimental results of the position controlled linear motor by using the traditional observers when the impulse disturbance is added.

Moreover, the impulse disturbance (100 μsec width, maximum motor torque) is added for every 210 $m$sec during the position control. The performance of the controlled motor employing the new nonlinear disturbance observer is better (about 35%) than that employing the traditional disturbance observer. Figure 4.18 shows the experiment results where the new disturbance observer and new speed observer are used. Figure 4.19 shows the experiment results where the traditional disturbance observer and traditional speed observer are used. The desired position $y_m(t)$ (2.5 [cm]/div) in the top of the two figures are same. The signals in the middle of the two figures are the tracking errors (1×10^{-2}[cm]/div). The signals in the bottom show the estimated speeds $s\hat{y}(t)$ (6.7[cm/s]/div).

4.11 Conclusions

In this chapter, based on the VSS equivalent control method, the disturbance observer is constructed for the minimum phase as well as nonminimum phase (by using

approximate inverse systems) dynamical systems with arbitrarily relative degrees. Here the term "disturbance" is referred to the combination of the model uncertainties, the nonlinear parts of the system and the external disturbances. Only the upper and lower bounds of the disturbances is assumed as the *a priori* information.

By choosing small design parameters δ_i $(1 \le i \le r)$ and λ, the performance of the new observer may become better even for the high frequency disturbances. But there is a limitation about the choice of these parameters when the measurement noises are present. When it is implemented by a digital computer, the design parameters are also limited by the sampling period. For the class of nonminimum phase systems, the parameter γ should be chosen large in order to get a good estimation.

The estimated disturbance is employed to formulate a state observer and to synthesize a pole assignment controller. Simulation results show that the proposed observer is of high robustness to the types of the disturbances and the model uncertainties. Experimental results show the new observer is of high practicality. Moreover, when the impulse disturbances exist, the experiment results show that the new observer is superior to the traditional disturbance observer.

For the systems with relatively large stochastic disturbances or measurement noises, the proposed disturbance observers should be modified. The proposed formulation is expected to be extended to the general nonminimum phase systems as well as much more complicated systems, such as the uncertain systems with delays, descriptor systems, affine parameter-dependent models, etc.

Chapter 5

VSS Theory-Based Disturbance Estimation Scheme and Its Applications for MIMO Systems

5.1 Introduction

Variable structure control systems are an established method of controlling uncertain dynamical systems and have been the focus of much research. Especially, their robust properties are well documented in [9,26,57]. But the main developments in this area are under the assumption that all the internal states are available to the control law. Of course, this is often not the case in practice. One way of overcoming this difficulty is to generate an estimate of the unavailable internal state. VSS type approaches are put forward by several authors [11,59-61,68]. The proposed observer systems are designed to provide asymptotic error decay in the presence of matched uncertainties. But all of the results are subjected to the minimum phase systems (with respect to the relation between the disturbance and the output) with the assumption that, from the point of view of state space, the partial states directly affected by the disturbances must directly appear in the outputs (For SISO system, this assumption is equivalent to that the system is minimum phase with relative degree one. From now on, we will also call this kind of MIMO systems "MIMO minimum phase dynamical systems with relative degree one".). An